Development 140, 43-55 (2013) doi:10.1242/dev.085290

Otx2 is an intrinsic determinant of the embryonic stem cell state and is required for transition to a stable epiblast stem cell condition

Dario Acampora[1,2], Luca G. Di Giovannantonio[1,2] and Antonio Simeone[1,2,*]

SUMMARY

Mouse embryonic stem cells (ESCs) represent the naïve ground state of the preimplantation epiblast and epiblast stem cells (EpiSCs) represent the primed state of the postimplantation epiblast. Studies have revealed that the ESC state is maintained by a dynamic mechanism characterized by cell-to-cell spontaneous and reversible differences in sensitivity to self-renewal and susceptibility to differentiation. This metastable condition ensures indefinite self-renewal and, at the same time, predisposes ESCs for differentiation to EpiSCs. Despite considerable advances, the molecular mechanism controlling the ESC state and pluripotency transition from ESCs to EpiSCs have not been fully elucidated. Here we show that Otx2, a transcription factor essential for brain development, plays a crucial role in ESCs and EpiSCs. Otx2 is required to maintain the ESC metastable state by antagonizing ground state pluripotency and promoting commitment to differentiation. Furthermore, Otx2 is required for ESC transition into EpiSCs and, subsequently, to stabilize the EpiSC state by suppressing, in pluripotent cells, the mesendoderm-to-neural fate switch in cooperation with BMP4 and Fgf2. However, according to its central role in neural development and differentiation, Otx2 is crucially required for the specification of ESC-derived neural precursors fated to generate telencephalic and mesencephalic neurons. We propose that Otx2 is a novel intrinsic determinant controlling the functional integrity of ESCs and EpiSCs.

KEY WORDS: Embryonic stem cells, Epiblast stem cells, Neural fate, Otx2

INTRODUCTION

Understanding the genetic and epigenetic mechanisms that control the initial state and differentiation capability of pluripotent stem cells is essential for the comprehension of mammalian development and for the design of experimental protocols for the controlled generation of cell types of therapeutic interest (Hanna et al., 2010; Rossant, 2008; Murry and Keller, 2008; Niwa, 2007). Mouse embryonic stem cells (ESCs) have been isolated from the inner cell mass (ICM) of the blastocyst, may generate chimeric embryos at high efficiency, and their undifferentiated state depends on a self-maintaining network of core transcription factors [Oct4 (Pou5f1), Sox2, Nanog and Klf4/2/5] and signaling pathways (LIF, WNT and BMP4), which ensure self-renewal and protection from FGF-mediated lineage commitment (Silva and Smith, 2008; Lanner and Rossant, 2010; Hanna et al., 2010; Silva et al., 2009; Chambers et al., 2007; Niwa, 2011; Niwa et al., 2009; Ying et al., 2008; Ying et al., 2003a; Wray et al., 2011; Yi et al., 2011; Lyashenko et al., 2011; ten Berge et al., 2011; Nichols et al., 2009; Matsuda et al., 1999). The ESC population is not homogeneous, but rather is characterized by cell-to-cell spontaneous and reversible differences in the expression level and sensitivity to specific transcription factors and signaling pathways, which together maintain the balance between self-renewal and susceptibility to differentiation. This condition has been defined as the metastable state of ESCs (Niwa et al., 2009; Miyanari and Torres-Padilla, 2012; Niwa, 2007; Silva and Smith, 2008; Silva et al., 2009; Chambers et al., 2007; Toyooka et al., 2008).

Mouse epiblast stem cells (EpiSCs) are derived from the epiblast of pre-streak embryos, express Oct4, Sox2 and Nanog (at a low level compared with ESCs) but are silent for Klf factors, exhibit specific markers such as *Fgf5* and brachyury (T), are highly inefficient in chimera formation and their self-renewal and undifferentiated states depend on FGF and activin A signaling pathways (Hanna et al., 2010; Lanner and Rossant, 2010; Brons et al., 2007; Tesar et al., 2007; Najm et al., 2011). However, most of these signaling factors have several functions; for example, FGF signaling is also required to inhibit neural differentiation of EpiSCs and to prevent their reversion to a preimplantation ESC-like state, and BMP4 is required to suppress neural fate and allow differentiation toward non-neural lineages (Lanner and Rossant, 2010; Greber et al., 2010; Greber et al., 2011; LaVaute et al., 2009; Kunath et al., 2007; Zhang et al., 2010; Di-Gregorio et al., 2007; Linker and Stern, 2004).

The ESC state corresponds to the naïve ground state of the preimplantation epiblast, whereas the EpiSC state corresponds to the primed state of the postimplantation epiblast (Hanna et al., 2010; Niwa, 2007; Lanner and Rossant, 2010; Nichols and Smith, 2009), thus implying that ESCs should be converted to a primed epiblast-like state before definitive differentiation into germ layers occurs. However, despite significant advancements, the regulatory mechanisms that control the state and differentiation capability of ESCs and EpiSCs remain to be fully clarified. Here, we have studied whether the transcription factor Otx2, which is required at multiple steps in brain development and neuronal differentiation (Simeone et al., 1992; Simeone et al., 2002; Simeone et al., 2011), might be functionally relevant in ESCs and EpiSCs, where it is expressed. We found that Otx2 is crucially required to maintain the ESC metastable state by opposing self-renewal and predisposing

[1]CEINGE Biotecnologie Avanzate, Via G. Salvatore 486, 80145 Naples, Italy and SEMM European School of Molecular Medicine – Naples site, Italy. [2]Institute of Genetics and Biophysics 'Adriano Buzzati-Traverso', CNR, Via P. Castellino 111, 80131 Naples, Italy.

*Author for correspondence (simeone@ceinge.unina.it)

Accepted 2 October 2012

the cells to differentiation. Moreover, Otx2 stabilizes the transition from naïve ESCs to primed EpiSCs in cooperation with BMP4 and Fgf2 and is required for telencephalic and mesencephalic differentiation of ESC-derived neural progenitors.

MATERIALS AND METHODS

Generation of ESC lines

The ESC lines were generated in E14Tg2a cells. In the *Otx2*$^{-/-}$ ESC line, the coding exons of *Otx2* alleles have been replaced with *lacZ* and *GFP* (Acampora et al., 1995; Acampora et al., 2009) (supplementary material Fig. S1A-C). In the *R26*$^{Otx2/Otx2}$ ESC line, a cassette including full-length *Otx2* coding cDNA followed by an IRES *GFP* sequence is inserted into the *Rosa26* locus (Di Salvio et al., 2010) (supplementary material Fig. S1D-G). The *Otx2*$^{-/-}$;*R26*$^{GFP/+}$ ESC line carries an *Otx2*$^{floxed\text{-}out}$ null allele and the *Otx2*^{lacZ} null allele; in addition, the *GFP* gene was inserted into the *Rosa26* locus for chimerism studies (supplementary material Fig. S1H-O). The *R26*$^{GFP/+}$ ESC line carries the *GFP* gene in the *Rosa26* locus and was used as control for chimerism experiments (supplementary material Fig. S1M-O). The *Otx2*$^{flox/-}$;*R26*$^{CreER/+}$ ESC line carries an *Otx2*^{flox} allele in combination with the *Otx2*^{lacZ} null allele (*Otx2*$^{flox/-}$). An inducible *CreER-puro* cassette was introduced into the *Rosa26* locus (supplementary material Fig. S1P-S).

ESC differentiation

Serum-free floating embryoid body-like aggregates (SFEBs) were generated from ESCs as reported (Watanabe et al., 2005). Mesendoderm differentiation in adherent conditions was obtained under serum-free conditions in the presence of activin A for 4 days (d) (Waese and Stanford, 2011; Izumi et al., 2007). For neural differentiation, SFEBs were cultured up to d5 without exogenous factors or with Dkk1 (from d1 to d5) (R&D Systems; 500 ng/ml), followed by adherent culture for 5 more days (Watanabe et al., 2005); alternatively, neural differentiation was induced using adherent monoculture conditions (Ying et al., 2003b).

ESC transfection

Otx2$^{-/-}$ ESCs were transfected using Lipofectamine 2000 reagent (Invitrogen) with a plasmid overexpressing *Otx2* cDNA under a CMV-chicken β-actin promoter (CAG). Six hours after transfection, ESCs were seeded in ESC medium or differentiated into SFEBs.

ESC-derived and embryo-derived EpiSCs

ESCs were seeded at a density of 3×10^3/cm^2 in N2B27 supplemented with 20 ng/ml activin A (R&D Systems) and 12 ng/ml Fgf2 (Peprotec) and cultured for 6 days (Brons et al., 2007; Tesar et al., 2007; Zhang et al., 2010), which corresponded to passage (p) 0. For further passages, EpiSCs were cultured in the same conditions. For Otx2 conditional inactivation, *Otx2*$^{flox/-}$;*R26*$^{CreER/+}$ EpiSCs were administered with 4-hydroxy-tamoxifen (4-OHT) (125 nM) at p1 and kept in 40 nM 4-OHT throughout subsequent passages. Epiblasts were dissected from single embryonic day (E) 5.75 mouse embryos and incubated in EpiSC medium.

Growth factors and cytokine assays

LIF and FGF response was monitored as previously described (Mitsui et al., 2003; Zhang et al., 2010). For experiments involving BMP4 (recombinant human; R&D Systems), the factor was administered on d1 to ESC- or EpiSC-derived SFEBs (Zhang et al., 2010) at 0.5 and 10 ng/ml; SFEBs were then cultured up to d5. EpiSCs induced with Fgf2 and activin A were also administered with BMP4 (10 ng/ml) at p1 and until p4. Experiments involving activation or inhibition of the FGF and BMP pathways were performed in three conditions: (1) ESCs kept in 15% knockout serum replacement (KSR) medium with LIF were administered with BMP4 (10 ng/ml) or Fgf2 (12 ng/ml) or the BMP inhibitor dorsomorphin (DM) (0.5 μM; Calbiochem) or the Fgf/Erk inhibitor PD325901 (PD) (1 μM; Calbiochem) or with both inhibitors for 12 hours; (2) ESCs kept in ESC medium were cultured for the last 12 hours in 5% KSR medium plus BMP4 or Fgf2 or their inhibitors; (3) EpiSCs in N2B27 containing Fgf2 and activin A were cultured for 12 hours in N2B27 plus activin A only or also supplemented with BMP4 or DM, PD, or DM plus PD.

Alkaline phosphatase (ALP) assays and LIF dependence experiments

ALP staining was performed on EpiSCs at p0 and later passages or on ESCs in three different growth conditions at clonal density (1×10^3 cells/10 cm^2): in ESC medium (with LIF), without LIF, or without LIF plus JAK inhibitor 1 (0.6 μM; Calbiochem). ALP activity was revealed by the naphthol/Fast Red Violet reaction.

EpiSCs derived from SFEBs

SFEBs treated with BMP4 (10 ng/ml) from d1 were trypsinized at d2 and reseeded in EpiSC medium (without BMP4) at a cell density of 1×10^5/10 cm^2. Immunostaining for Oct4 was performed on d6 to unambiguously identify EpiSC colonies.

Chimeras and teratomas

Chimeras were obtained by injecting 13-16 ESCs or *Otx2*$^{-/-}$ EpiSCs into C57BL/6 blastocysts and colonization was evaluated by assessing GFP expression on E11.5, E9 or E8. Teratomas were generated by subcutaneous injection of 1.5×10^6 ESCs or EpiSCs into NOD SCID mice. For *Otx2*$^{-/-}$ ESCs, teratoma occurrence was also assayed by injecting 6×10^6 ESCs.

Immunohistochemistry

SFEBs and postimplantation mouse embryos were embedded in paraffin and processed as described (Acampora et al., 2009). For immunohistochemistry on ESCs and EpiSCs cultured on Permanox chamber slides, paraformaldehyde-fixed cells were blocked in 2% skimmed milk powder and 0.3% Triton X-100. Morulae and blastocysts were blocked in 1% BSA, 10% FBS and 0.2% Triton X-100. Antibodies raised in rabbit were directed against Otx2 (1:3500), Sox2 (1:500) (both gifts of G. Corte, CBA, Geneva), Nanog (1:600; Calbiochem), Foxa2 (1:1000; Abcam), Foxg1 (1:500) and Eomes (1:1000) (Chemicon); antibodies raised in goat were against Otx2 (1:100; R&D Systems), Sox1 (1:100; Santa Cruz Biotechnology), T (1:150; Santa Cruz Biotechnology) and GFP (1:200; Abcam); antibodies raised in mouse were against Oct4 (1:250; Santa Cruz Biotechnology), Cdx2 (1:5; BioGenex), nestin (1:1000; Chemicon), Pax6 (1:150; Developmental Studies Hybridoma Bank), Nkx2.1 (1:200; Santa Cruz Biotechnology), αMHC (1:500; Developmental Studies Hybridoma Bank), Gfap (1:200; Chemicon) and Tuj1 (Tubb3 – Mouse Genome Informatics) (1:5000; Covance). Propidium iodide or DAPI counterstaining was performed as necessary.

RT-PCR and western blotting

RT-PCR was performed in non-saturating conditions using the primers and cycles listed in supplementary material Table S1. Western blots were probed with rabbit antibodies against Erk1,2 (Mapk3/1 – Mouse Genome Informatics) (1:1500), p-Erk1,2 (1:350), Stat3 (1:1000), p-Stat3 (1:350), Smad1 (1:1000), p-Smad1,5,8 (1:350) (Cell Signaling); β-actin antibody (1:6000; Sigma) was raised in mouse.

Cell counting and statistical analysis

Cell counting was performed manually on immunohistochemistry images printed in A4 format or using ImageJ software (NIH). Standard deviation was calculated from four independent experiments.

RESULTS

Otx2 is expressed in preimplantation and early postimplantation embryos, ESCs and EpiSCs

In preimplantation mouse embryos, Otx2 was expressed in late morula blastomeres co-expressing Nanog or the trophectoderm determinant Cdx2 and, during blastocyst development, Otx2 colocalized with Cdx2 in trophectoderm and with Nanog in a fraction of cells of the ICM (Fig. 1A). Upon embryo implantation, robust Otx2 expression was detected in epiblast and visceral endoderm. At E6.5, Otx2 was downregulated in posterior epiblast, where the second wave of Nanog expression was activated (Fig. 1B). In ESCs, 46% of the Oct4$^+$ cells co-expressed Otx2, whereas only a fraction of Oct4$^+$ cells colocalized with Nanog and Klf4 (Fig. 2A-C). Cell counting on cytospun ESCs showed that

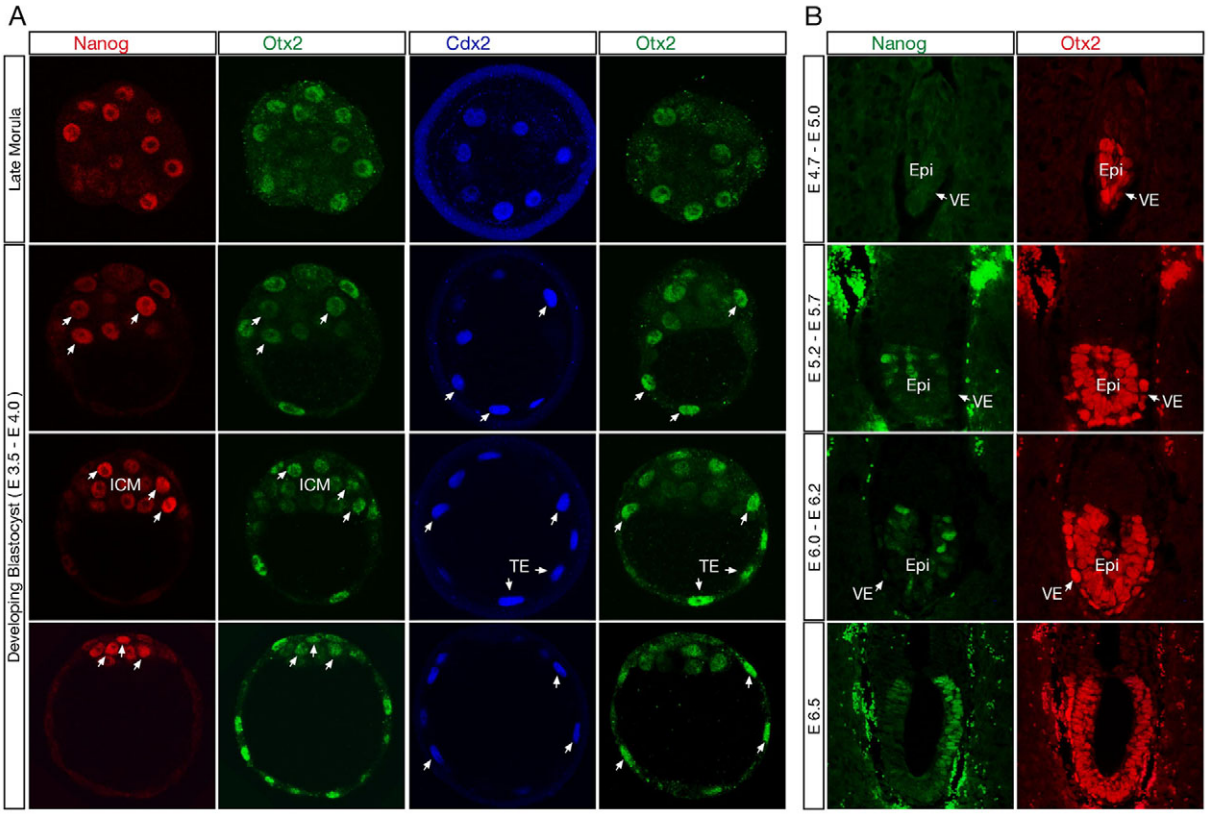

Fig. 1. Otx2 expression in preimplantation and early postimplantation mouse embryos. (**A**) Co-immunohistochemistry for Otx2 and Nanog and for Cdx2 and Otx2 in late morula embryos and during blastocyst development. (**B**) Co-immunohistochemistry for Otx2 and Nanog in early postimplantation embryos up to early streak stage. The arrows in A point to Nanog$^+$ Otx2$^+$ ICM cells and Otx2$^+$ Cdx2$^+$ TE cells. ICM, inner cell mass; TE, trophectoderm; Epi, epiblast; VE, visceral endoderm.

Otx2$^+$ cells were almost equally distributed between those expressing high or moderate levels of Nanog and those with low or no expression of Nanog (Fig. 2D-G; supplementary material Table S2). Moreover, ESCs exhibiting high levels of Otx2 preferentially expressed low levels of Nanog, whereas those with low levels of Otx2 exhibited high Nanog expression (Fig. 2D-G). In EpiSCs, Otx2 was detected in all Oct4$^+$ cells at a level that varied between cells and was frequently complementary to that of Nanog (Fig. 2H). These data indicate that Otx2 is a molecular correlate of different pluripotent cell types *in vivo* and *in vitro*.

Otx2 is an early responding factor to ESC differentiation

ESC differentiation may be activated by LIF withdrawal and/or low concentrations of serum, and early postimplantation embryonic development can be mimicked by ESC-derived embryoid bodies. In these culture conditions, Otx2 expression was highly responsive to ESC differentiation. Indeed, LIF withdrawal and/or diminished concentrations of KSR medium induced a rapid and generalized activation of Otx2 and a corresponding reduction in the number of Nanog$^+$ ESCs (supplementary material Fig. S2A-D). Similarly, in differentiating SFEBs, Otx2 rapidly spread to all the Oct4$^+$ cells, mirrored the downregulation of Nanog, *Klf4* and *Rex1* (*Zfp42* – Mouse Genome Informatics), and anticipated the induction of the epiblast markers *Fgf5* and *Cer-l* (*Cer1* – Mouse Genome Informatics) and the generation of T$^+$ primitive streak-like and Sox1$^+$ neural cells (supplementary material Fig. S2E-H, Table S3). These observations support the possibility that Otx2 is required in ESCs to control their state and/or promote their differentiation.

Otx2 is required to maintain the ESC state

To investigate the role of Otx2 we generated mutant ESC lines that lack (*Otx2*$^{-/-}$) or ubiquitously and constitutively express (*R26*$^{Otx2/Otx2}$) *Otx2* (supplementary material Fig. S1). First, we studied functional parameters and markers related to the undifferentiated state or predisposition to differentiation. Compared with wild type (wt), virtually all the *Otx2*$^{-/-}$ ESC colonies exhibited a sphere-like morphology, uniform ALP staining, ubiquitous distribution of Nanog and Klf4 and higher expression of *Rex1* (Fig. 3A-D; supplementary material Tables S4, S5). During the earliest stages of wt ESC colony formation, Otx2 and Nanog exhibited complex expression profiles with variable degrees of complementarity, whereas *Otx2*$^{-/-}$ ESC colonies exhibited constitutively high expression of Nanog (supplementary material Fig. S3). These data suggest that, in the absence of Otx2, the fluctuating expression of Nanog is severely affected and, therefore, that Otx2 is directly or indirectly required to prevent its constitutive expression.

In *Otx2*$^{-/-}$ ESCs, the endogenous activities of LIF and FGF were respectively enhanced and severely decreased, as monitored by the level of the phosphorylated, active forms of the LIF signaling transcriptional mediator Stat3 (p-Stat3) and the extracellular signal-related kinases 1 and 2 (p-Erk1,2)

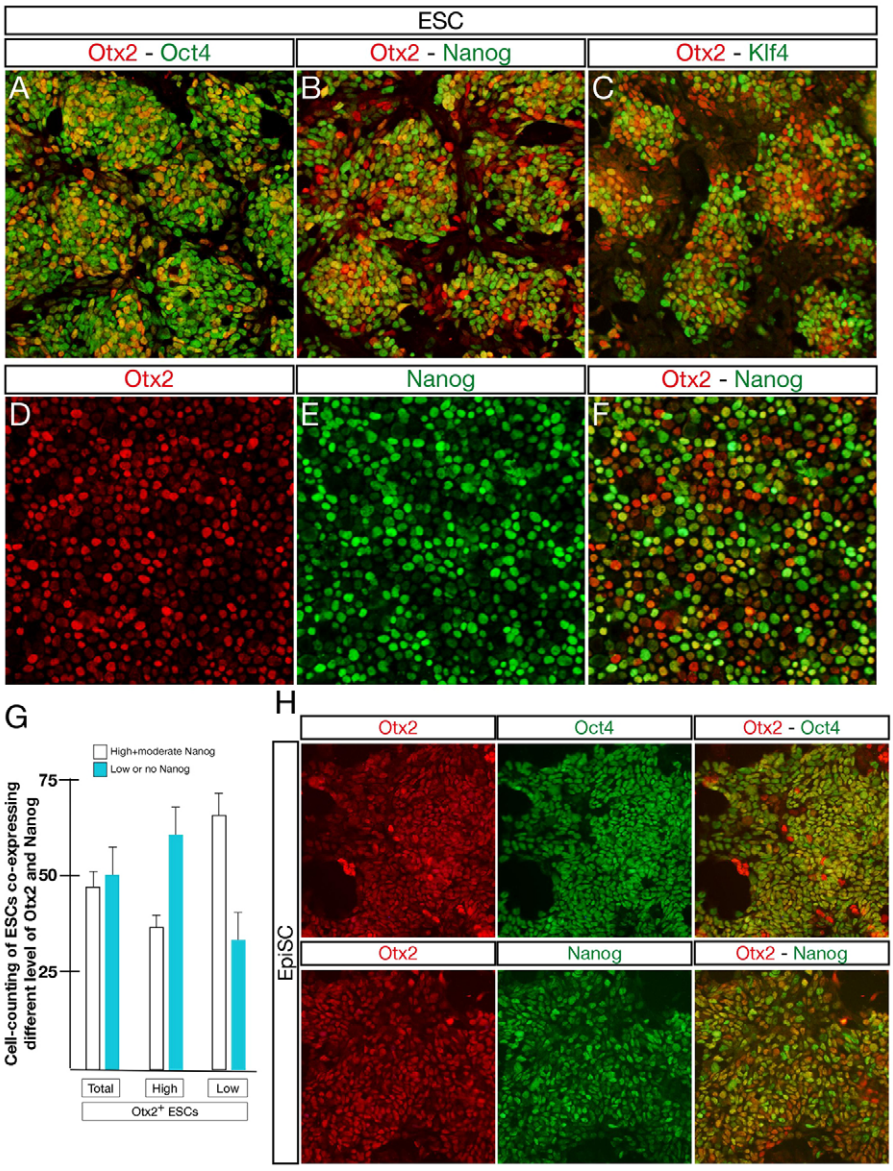

Fig. 2. Otx2 expression in ESCs and EpiSCs. (**A-C**) Immunohistochemistry showing that in ESCs Otx2 is co-expressed with Oct4 (A) and only with a fraction of cells expressing Nanog and/or Klf4 (B,C). (**D-G**) Cell counting of cytospun ESCs immunostained for Otx2 and Nanog (D-F) shows the percentage of total Otx2$^+$ cells (regardless of the Otx2 expression level) co-expressing high or low levels of Nanog (G); the cell counting also shows that ESCs with high levels of Otx2 preferentially co-express low levels of Nanog, whereas those exhibiting low levels of Otx2 co-express high levels of Nanog (G). Error bars indicate s.d. (**H**) Immunohistochemistry for Otx2 and Oct4 and for Otx2 and Nanog show that Otx2 is an EpiSC marker.

(Fig. 3E,F). Furthermore, compared with wt, LIF addition to LIF-deprived ESCs generated a substantially higher response in *Otx2*$^{-/-}$ ESCs (Fig. 3E), and LIF deprivation and blockade of Stat3 phosphorylation by JAK inhibitor 1 were not sufficient to disrupt the undifferentiated state of *Otx2*$^{-/-}$ ESCs (Fig. 3G,H; supplementary material Table S4). Since this phenotype may also depend on loss of autocrine Fgf4 activity (Kunath et al., 2007) or abnormal expression of NuRD complex components (Reynolds et al., 2012; Kaji et al., 2006), the expression of *Fgf4*, *Fgfr1-4*, *Mbd3*, *Mta1* and *Mta2*, *Rbap46* (*Rbbp7* – Mouse Genome Informatics) and *Hdac1* was analyzed, and showed a very mild reduction in *Otx2*$^{-/-}$ ESCs only for *Fgf4* (supplementary material Fig. S4).

Chimerism was studied using a second, independent *Otx2*$^{-/-}$ ESC line carrying a GFP constitutive reporter in the *R26* locus (supplementary material Fig. S1). Lack of Otx2 only impaired chimerism in the forebrain and midbrain (Fig. 4A-C), whereas the frequency and growth of *Otx2*$^{-/-}$ ESC-derived teratomas were substantially affected (Fig. 4D,E; supplementary material Tables S6, S7).

Next, we investigated whether ubiquitous and constitutive expression of Otx2 was sufficient to affect the ESC state by promoting differentiation. *R26*$^{Otx2/Otx2}$ ESCs exhibited a fairly flat morphology, a low frequency of uniformly ALP-stained colonies, a reduced percentage of ESCs co-expressing high levels of Nanog and Klf4, decreased expression of *Rex1* (Fig. 3A-D), a heavily attenuated response to LIF and substantially enhanced activity of endogenous FGF (Fig. 3E,F). Remarkably, *R26*$^{Otx2/Otx2}$ ESCs exhibited the typical signature of primed EpiSCs, such as the expression of *Fgf5* and *Cer-l*, generation of T$^+$ cells (Fig. 3A,D) and very poor ability to generate chimeras, while retaining high efficiency in teratoma formation (Fig. 4A,C-E). Thus, Otx2 ubiquitous expression in ESCs is sufficient to induce stable molecular and functional features of the EpiSC state.

Collectively, these findings suggest that Otx2 is required to maintain the integrity of the ESC state by controlling the dynamic balance between pluripotency with high self-renewal and susceptibility to differentiation (Fig. 3I). In this context, *Otx2*$^{-/-}$ ESCs resemble ESCs cultured in 2i, which exhibit severe downregulation of Otx2 (Marks et al., 2012).

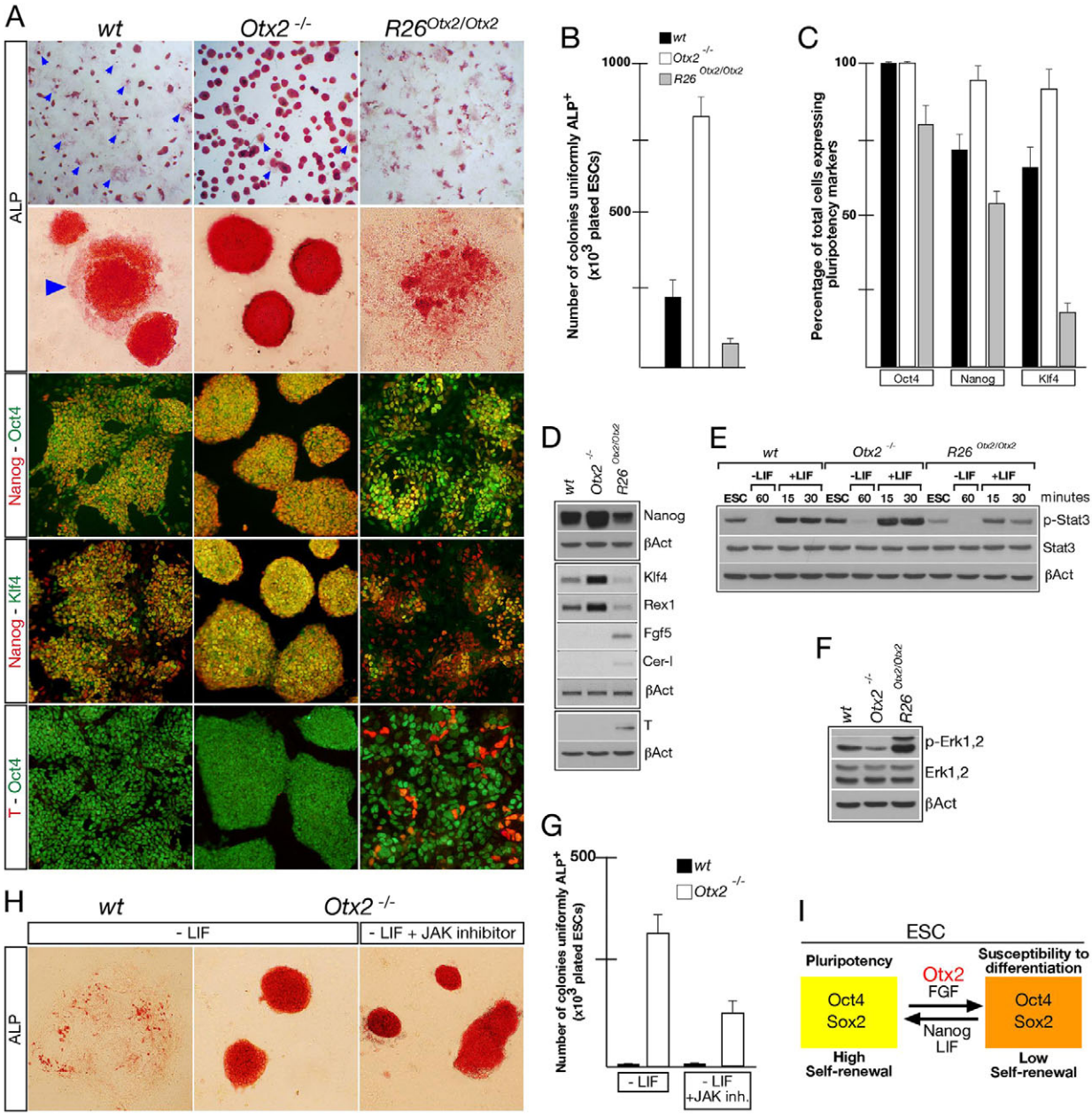

Fig. 3. Maintenance of the ESC state depends on Otx2. (**A-D**) Compared with wt, virtually all of the *Otx2*$^{-/-}$ ESC colonies show uniform ALP staining (A,B), ubiquitous high expression of Nanog and Klf4 (A,C,D) and increased levels of *Rex1* transcripts (D); conversely, *R26*$^{Otx2/Otx2}$ ESCs show decreased numbers of colonies with uniform ALP staining (A,B), a diminished percentage of total cells expressing Oct4, Nanog or Klf4 (A,C), low expression of *Rex1* (D) and activation of the epiblast markers *Fgf5*, *Cer-l* and T (A,D). Arrowheads (A) point to ESC colonies that are not uniformly ALP^{+}. (**E**) Compared with wt, *Otx2*$^{-/-}$ and *R26*$^{Otx2/Otx2}$ ESCs respectively exhibit higher and lower endogenous LIF activity as revealed by p-Stat3 level; when stimulated with LIF after 60 minutes of LIF deprivation, the p-Stat3 level is substantially increased in *Otx2*$^{-/-}$ and attenuated in *R26*$^{Otx2/Otx2}$ ESCs. (**F**) Compared with wt ESCs, the endogenous FGF activity revealed by p-Erk1,2 is diminished in *Otx2*$^{-/-}$ and substantially increased in *R26*$^{Otx2/Otx2}$ ESCs. (**G**,**H**) LIF deprivation, or LIF deprivation in the presence of JAK inhibitor 1, is not sufficient to abolish self-renewal (G) and ESC colonies continue to exhibit uniform ALP staining (H). β-actin was used to normalize western blots (E,F, Nanog and T in D) and RT-PCRs (*Klf4*, *Rex1*, *Fgf5* and *Cer-l* in D). Error bars indicate s.d. (**I**) The ESC state is characterized by dynamic and reversible fluctuations between ESCs with high self-renewal and those with reduced self-renewal that are poised to become postimplantation epiblast. Antagonism driving the metastable ESC state is primarily controlled by FGF and LIF signaling activities together with Nanog. Our results suggest that Otx2 is a novel component of this circuit, being required to maintain the metastable ESC condition by opposing high self-renewal and promoting predisposition to differentiation.

Otx2 is required for ESC conversion into EpiSCs

We then studied Otx2 requirement in ESC differentiation by monitoring sequential steps marking pluripotency transition from ESCs to EpiSCs. First, we analyzed the response to Fgf2, which primes ESC differentiation. Compared with wt, *Otx2*$^{-/-}$ ESCs showed a severe reduction in the p-Erk1,2 level, whereas in *R26*$^{Otx2/Otx2}$ ESCs, which already exhibited strong endogenous FGF activity, the response to Fgf2 was substantially higher (Fig. 5A). In

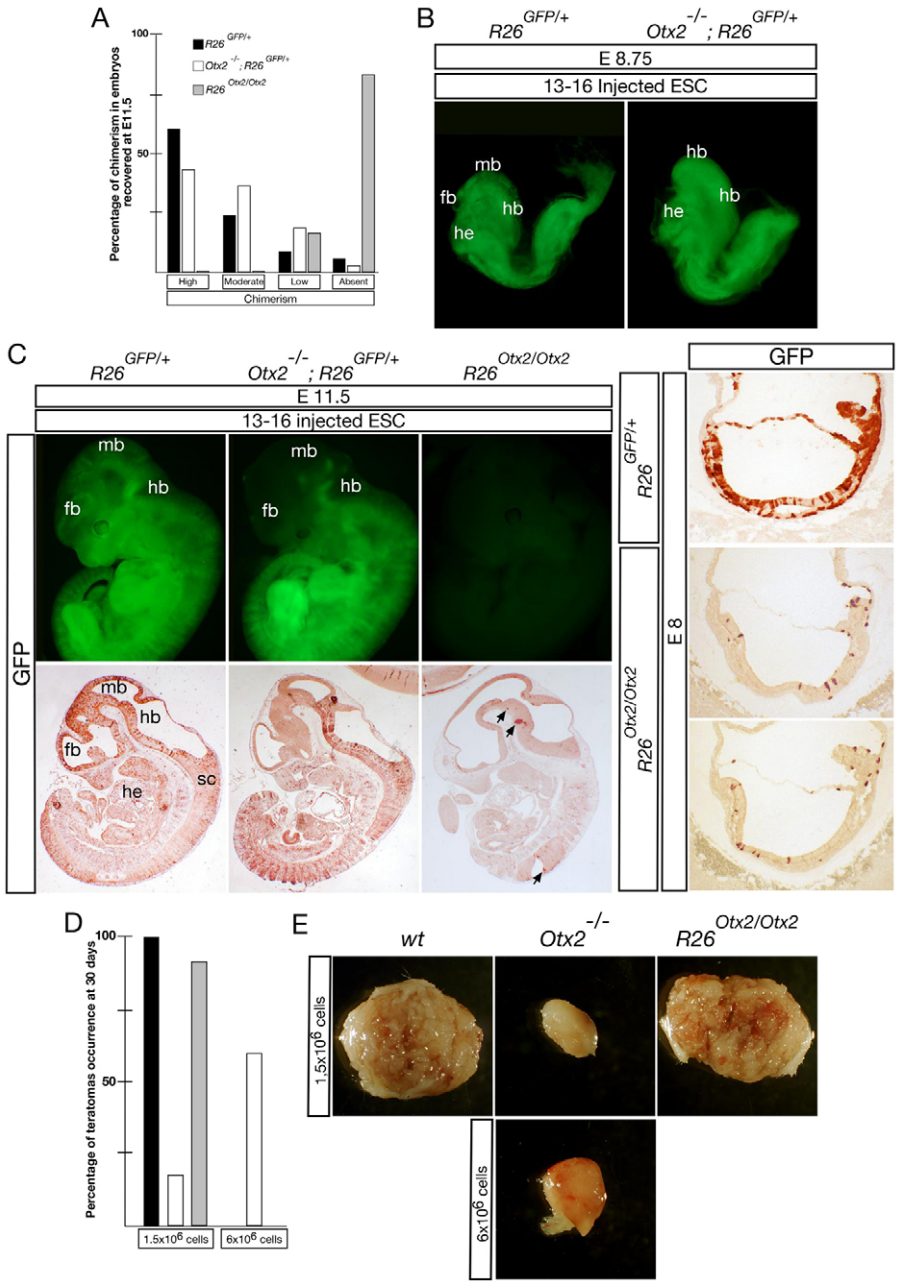

Fig. 4. Chimerism and teratoma formation. (**A-C**) GFP fluorescence and immunohistochemistry show that the efficiency in generating chimeric embryos is very similar for $R26^{GFP/+}$ and $Otx2^{-/-};R26^{GFP/+}$ ESCs, and is substantially affected for $R26^{Otx2/Otx2}$ ESCs, even when scoring E8 embryos (A,C). Note that highly chimeric embryos injected with $Otx2^{-/-};R26^{GFP/+}$ cells exhibit a typical headless phenotype (B), whereas in those that are less chimeric, $Otx2^{-/-}$ ESCs fail to colonize forebrain and midbrain (C). Arrows (C) point to isolated patches of $R26^{Otx2/Otx2}$ ESCs. (**D**,**E**) The frequency of teratoma occurrence (D) and their growth (E) are severely affected in $Otx2^{-/-}$ ESCs, whereas these parameters are similar for $R26^{Otx2/Otx2}$ and control ESCs. fb, forebrain; mb, midbrain; hb, hindbrain; sc, spinal cord; he, heart.

the absence of any growth factor or cytokine, $Otx2^{-/-}$ differentiating SFEBs showed after d1 a rapid loss of $Oct4^+$ cells, failed to efficiently downregulate Nanog, Klf4 and *Rex1*, did not activate *Fgf5* and *Cer-l*, and prematurely differentiated exclusively into $Sox1^+$ neural cells co-expressing nestin and Sox2 (Fig. 5B-D; supplementary material Fig. S5A, Tables S3, S8). Conversely, $R26^{Otx2/Otx2}$ SFEBs showed a more graded decrease of $Oct4^+$ cells, efficiently repressed Nanog, Klf4 and *Rex1*, expressed high levels of *Fgf5* and *Cer-l* over the entire timecourse and differentiated prevalently into T^+ primitive streak-like cells (Fig. 5B-D; supplementary material Fig. S5A, Tables S3, S8). Compared with d3.5 control SFEBs, these $R26^{Otx2/Otx2}$ SFEBs exhibited a substantial increase in the number of $Sox1^-$ $Foxa2^+$ cells (Fig. 5D), which are likely to correspond to T^+ cells generated before d3.5 and differentiated into endoderm. Further mesendoderm determinants, such as *Mixl1*, *Eomes*, *Gsc* and *Tbx6* (Izumi et al., 2007), showed that, as for T, their expression was virtually lost in $Otx2^{-/-}$ SFEBs (supplementary material Fig. S5B). Thus, in the absence of any added factor, Otx2 is required in ESCs to promote their exit from the undifferentiated state and to protect committed EpiSCs from a premature neural fate.

To better evaluate the pluripotency and lineage potential of *Otx2* mutant ESC lines, we analyzed $Otx2^{-/-}$ and $R26^{Otx2/Otx2}$ ESC-derived teratomas (n=3 per genotype). Compared with wt, *Otx2* mutant teratomas showed no obvious difference in the generation of neurons ($neurofilament^+$), glial cells ($Gfap^+$), muscle-like (αMHC^+) and endoderm-like ($Foxa2^+$) structures; however, $Otx2^{-/-}$ teratomas exhibited a widespread abnormal distribution of $Sox1^+$ $nestin^+$ neural rosette-like and $Oct4^+$ $Nanog^+$ pluripotent-like cell aggregates (supplementary material Fig. S6), suggesting that Otx2 prevents the accumulation of neural progenitors and pluripotent-like cells.

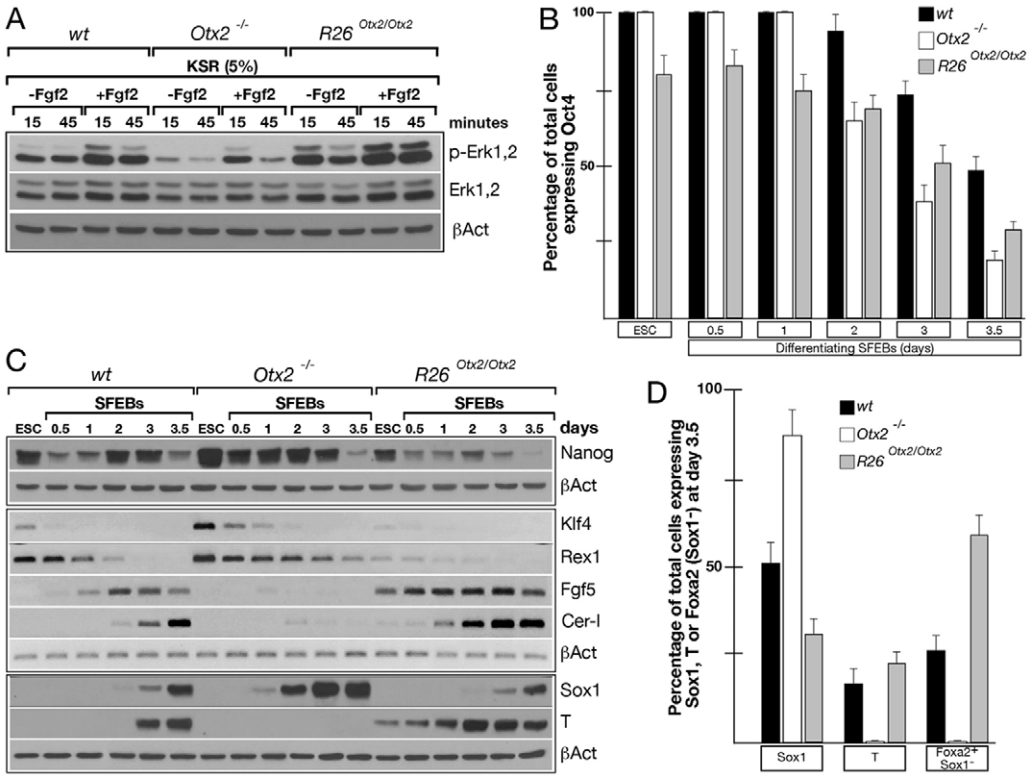

Fig. 5. Otx2 is required for ESC differentiation. (**A**) Compared with wt ESCs stimulated with Fgf2 after a brief starvation in 5% KSR, the response of *Otx2*$^{-/-}$ ESCs to Fgf2 is substantially affected, as revealed by the p-Erk1,2 level, and is even more pronounced for *R26*$^{Otx2/Otx2}$ ESCs, which already exhibit an elevated level of endogenous p-Erk1,2. (**B**) Oct4^{+} cell counts over the entire timecourse. (**C**) Expression analysis in wt, *Otx2*$^{-/-}$ and *R26*$^{Otx2/Otx2}$ differentiating SFEBs for Nanog, *Klf4*, *Rex1*, *Fgf5*, *Cer-l*, T and Sox1. β-actin is employed to normalize western blots and RT-PCRs (*Klf4*, *Rex1*, *Fgf5* and *Cer-l* in C). (**D**) Sox1^{+}, T^{+}, and Sox1^{-} Foxa2^{+} SFEB cell counts at d3.5. Error bars indicate s.d.

The phenotype of *Otx2*$^{-/-}$ ESCs is not caused by a secondary adaptive effect

To investigate whether the abnormalities described for *Otx2*$^{-/-}$ ESCs were caused by a secondary adaptive effect triggered by Otx2 ablation, we first analyzed whether reintroduction of Otx2 is sufficient to rescue some of the major phenotypic abnormalities and, second, inactivated Otx2 in a 4-OHT conditionally inducible ESC line (*Otx2*$^{flox/-}$;*R26*$^{CreER/+}$) (supplementary material Fig. S1). Immunostaining of Otx2 and Nanog in *Otx2*$^{-/-}$ ESCs transfected with a pCAG-Otx2 plasmid showed that most of the cells expressing high levels of Otx2 lacked or exhibited severely reduced expression of Nanog; moreover, d3.5 SFEBs generated after the pCAG-Otx2 transfection partially recovered the differentiation of T^{+} and Eomes^{+} cells (supplementary material Fig. S7A,B). In the second experiment, 48 hours after 4-OHT administration the *Otx2*$^{flox/-}$;*R26*$^{CreER/+}$ ESC colonies showed a compact morphology, ubiquitous expression of Nanog, increased levels of endogenous p-Stat3 and a moderate decrease in p-Erk1,2; SFEBs derived from 4-OHT-treated ESCs almost completely lacked T^{+} and Eomes^{+} cells (supplementary material Fig. S7C-E). Thus, the major phenotypes of *Otx2*$^{-/-}$ ESCs are not due to adaptive and irreversible effects triggered by Otx2 inactivation.

Otx2 stabilizes the EpiSC state

To investigate which, if any, of the Otx2 requirements described in differentiating SFEBs might be detected *in vivo*, we revisited the phenotype of *Otx2*$^{-/-}$ embryos. *Otx2*$^{-/-}$ embryos showed widespread derepression of Nanog in the epiblast of pre-gastrula and gastrulating embryos (Fig. 6A-C), while the generation of T^{+} cells, although delayed, was still efficient and premature differentiation of Sox1 neural progenitors was not observed (Fig. 6; data not shown) (Acampora et al., 2009; Acampora et al., 1995; Ang et al., 1996). We hypothesized that *in vivo*, with the exception of Nanog, embryonic extrinsic signals might circumvent abnormalities detected in *Otx2*$^{-/-}$ differentiating SFEBs. We examined whether *Otx2*$^{-/-}$ ESCs may be converted into EpiSCs when provided with Fgf2 and activin A, which promote ESC transition into EpiSCs and maintain their undifferentiated state. Moreover, FGF activity is required in EpiSCs also to suppress neuroectoderm differentiation and prevent regression to a preimplantation ESC-like state (Lanner and Rossant, 2010; Greber et al., 2010; Greber et al., 2011; Kunath et al., 2007).

Otx2$^{-/-}$ EpiSC colonies at p0, which corresponds to d6 of differentiation, showed spotted ALP staining and a mild increase in Sox1 expression but fairly normal expression of Nanog, *Fgf5*, *Cer-l* and T (supplementary material Fig. S8A-C). Suspecting these abnormalities as initial signs of a much more serious instability, *Otx2*$^{-/-}$ EpiSCs were analyzed at subsequent passages. Strikingly, at p5, *Otx2*$^{-/-}$ EpiSCs showed intense ALP staining and high levels of Nanog, mild reduction of *Fgf5* and *Cer-l* transcripts in *Oct4* normalized RNA samples, increased generation of Sox1^{+} nestin^{+} cells and a corresponding decrease of T^{+} cells (Fig. 7A,B). This phenotype worsened severely over time and, at p10, the great majority of *Otx2*$^{-/-}$ EpiSC colonies showed domed or sphere-like morphology with uniform ALP staining, strong Nanog immunoreactivity, severe decrease in *Fgf5* and *Cer-l* expression,

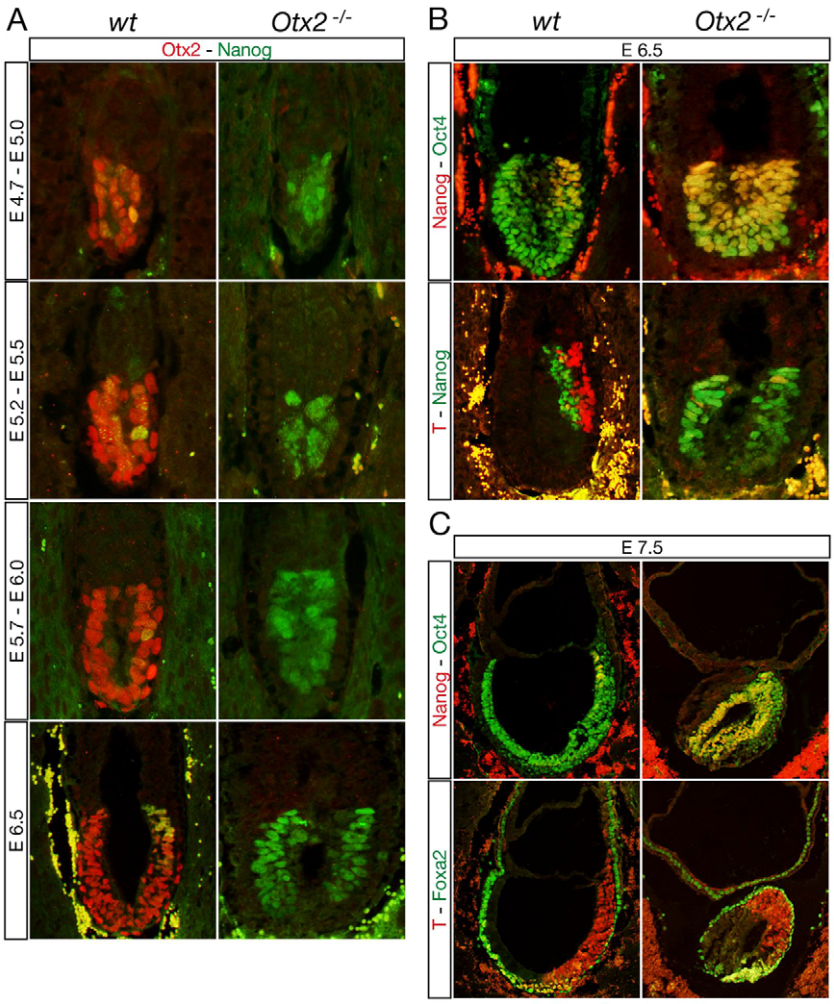

Fig. 6. *Otx2*$^{-/-}$ embryos exhibit Nanog but not Sox1 derepression. (**A**) Immunohistochemistry for Otx2 and Nanog on wt and *Otx2*$^{-/-}$ embryos shows that in early postimplantation *Otx2*$^{-/-}$ embryos the expression of Nanog is activated in most epiblast cells. (**B**,**C**) Immunohistochemistry for Oct4 and Nanog, T and Nanog, and T and Foxa2 on wt and *Otx2*$^{-/-}$ embryos at E6.5 (B) and E7.5 (C).

almost complete extinction of T^{+} cells, substantial reduction in the expression of *Eomes*, *Mixl1*, *Gsc* and *Tbx6*, and massive derepression of the neural lineage (Fig. 7A,B). However, p12 *Otx2*$^{-/-}$ EpiSCs can be propagated and maintained in EpiSC medium, thus excluding the possibility that they might have regressed to LIF dependence (data not shown). Accordingly, p5 *Otx2*$^{-/-}$*;R26*$^{GFP/+}$ EpiSCs failed to generate chimerism in E9 embryos (*n*=24; data not shown). However, p0 and p5 *Otx2*$^{-/-}$ EpiSCs were able to form teratomas and, as for those derived from *Otx2*$^{-/-}$ ESCs, they generated neuronal, glial, muscle-like and endodermal derivatives and numerous Sox1^{+} nestin^{+} rosette-like neural progenitors and Oct4^{+} Nanog^{+} cell aggregates (supplementary material Fig. S9, Table S7).

Next, we analyzed the effect of Otx2 ablation or constitutive expression following a different protocol using only activin A for mesendoderm differentiation (Waese and Stanford, 2011; Izumi et al., 2007), and found that lack of Otx2 primarily affected the expression of *Fgf5*, *Eomes*, *Mixl1*, *Gsc* and *Foxa2* and, interestingly, induced Sox1 and nestin in numerous Oct4^{+} patches; conversely, mesendoderm markers were all upregulated in *R26*$^{Otx2/Otx2}$ cells (supplementary material Fig. S10). Together, these data indicate that a high dosage of Fgf2 and activin A apparently compensates for the Otx2 requirement only for the initial transition of ESCs to primed EpiSCs, but not for maintenance of EpiSC identity. To assess whether Otx2 is an intrinsic stabilizer of the EpiSC state, we analyzed at p4 and p8 the phenotype of *Otx2*$^{flox/-}$*;R26*$^{CreER/+}$ conditional EpiSCs administered at p1 with 4-OHT, and found that they exhibited the same abnormalities described for *Otx2*$^{-/-}$ EpiSCs at similar passages (Fig. 7C-E). Of note, *Otx2*$^{flox/-}$*;R26*$^{CreER/+}$ EpiSC colonies that were not treated with 4-OHT also showed mild impairments at p8, suggesting an Otx2 dosage requirement for maintenance of the EpiSC state (Fig. 7C-E).

Finally, we tested our hypothesis that, *in vivo*, extrinsic factors might circumvent the requirement for Otx2 in EpiSCs. EpiSCs isolated from the egg cylinder of *Otx2*$^{-/-}$ embryos developed severe abnormalities that were undistinguishable from those of *Otx2*$^{-/-}$ ESC-derived EpiSCs (Fig. 7F). These findings indicate that Otx2 is an intrinsic determinant required to stabilize the EpiSC state by repressing the progressive switch of mesendoderm to neural fate and suggest that factor(s) other than, or together with, Fgf2 and activin A are required to stabilize the EpiSC state in cooperation with Otx2.

Otx2 functional interactions with Fgf2 and BMP4 for ESC transition to EpiSC and maintenance of the EpiSC state through suppression of neural fate

Previous studies have demonstrated that in ESCs BMP4 maintains pluripotency and antagonizes neural fate (Ying et al., 2003a; Zhang et al., 2010). Moreover, during embryoid body development, BMP4 first inhibits ESC transition into EpiSCs and, subsequently,

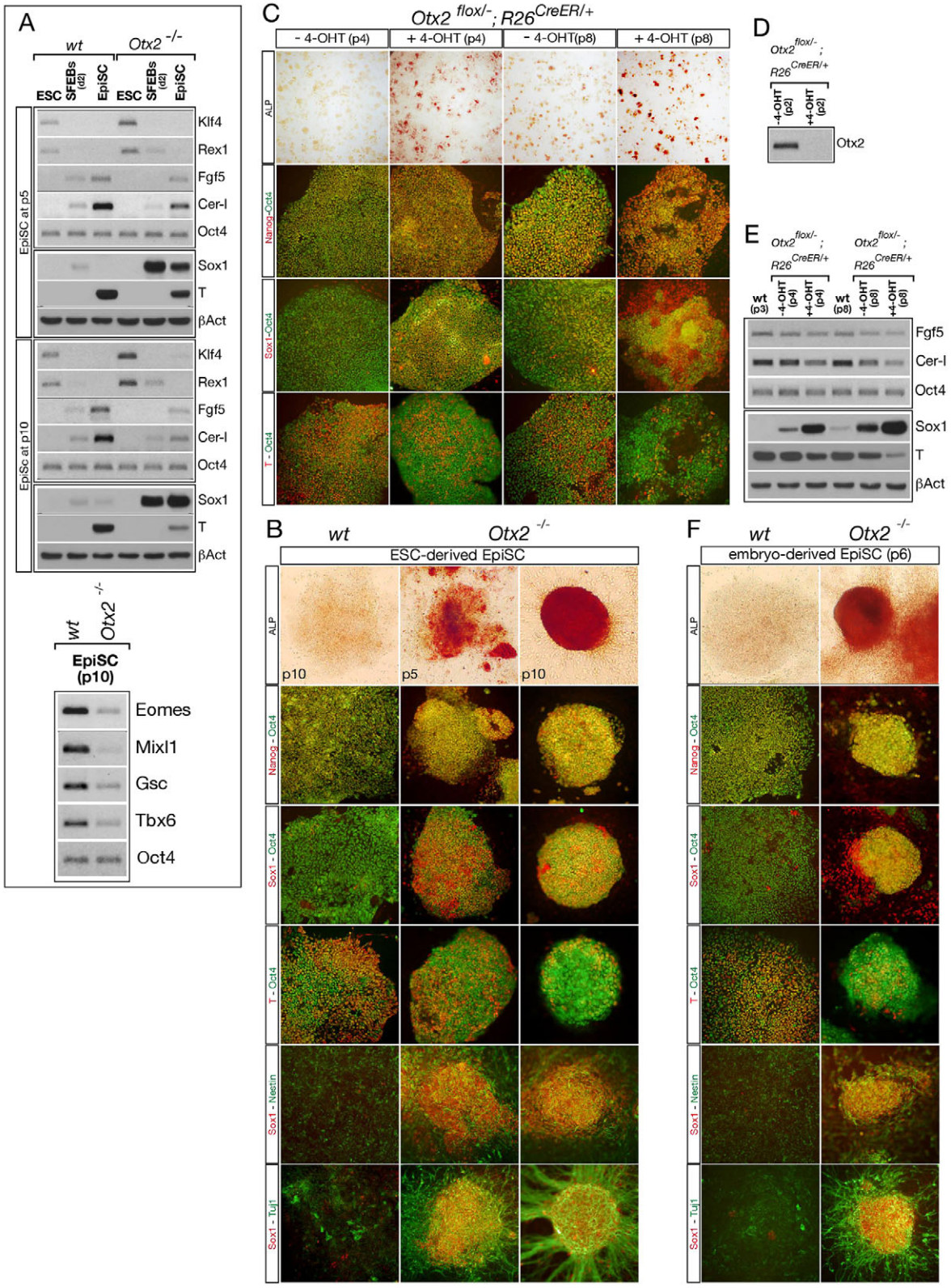

Fig. 7. Otx2 is required for maintenance of the EpiSC state. (**A**) Expression analysis of *Klf4*, *Rex1*, *Fgf5*, *Cer-l*, Sox1 and T markers in wt and *Otx2*$^{-/-}$ ESCs, d2 SFEBs, and EpiSCs at passage (p) 5 and p10, and expression of *Eomes*, *Mixl1*, *Gsc* and *Tbx6* mesendoderm markers in wt and *Otx2*$^{-/-}$ EpiSCs. (**B**) ALP reactivity and immunostaining on wt EpiSCs at p10 and *Otx2*$^{-/-}$ EpiSCs at p5 and p10 for Nanog and Oct4, Sox1 and Oct4, T and Oct4, Sox1 and nestin, and Sox1 and Tuj1. (**C**) ALP staining and immunohistochemistry for Nanog and Oct4, Sox1 and Oct4, and T and Oct4 on *Otx2*$^{flox/-}$;*R26*$^{CreER/+}$ EpiSCs untreated or treated at p1 with 4-OHT and analyzed at p4 and p8. (**D**,**E**) RT-PCR and western blot assays showing full inactivation of Otx2 at p2 (D) and expression of *Fgf5*, *Cer-l*, Sox1 and T at p4 and p8 (E). (**F**) *Otx2*$^{-/-}$ embryo-derived EpiSCs show at p6 a phenotype that is apparently identical to that of ESC-derived EpiSCs. RT-PCRs are normalized by *Oct4* and western blots by β-actin.

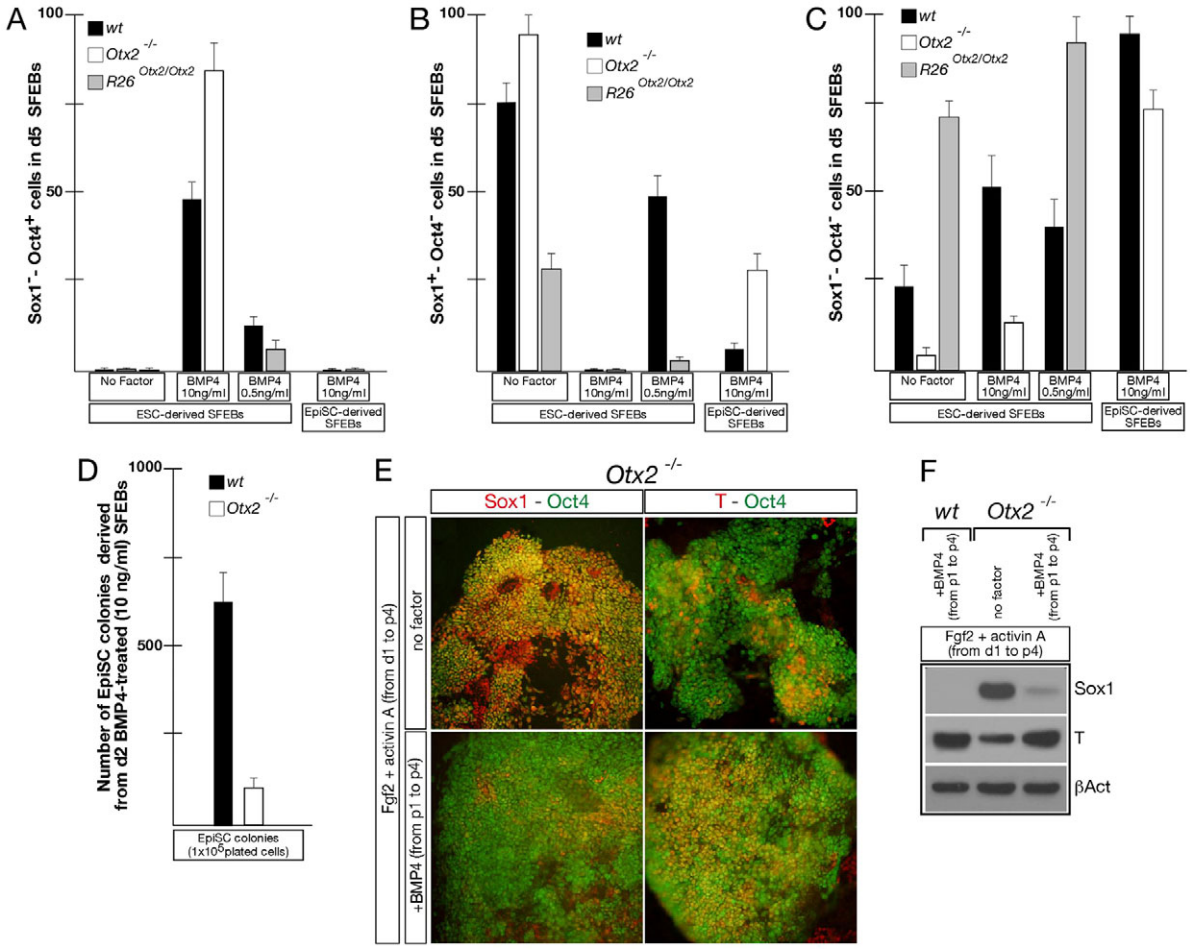

Fig. 8. Antagonism and synergism between BMP4 and Otx2 and cooperative recovery by BMP4 and Fgf2 of Otx2 requirement in EpiSCs. (**A-C**) Sox1$^-$ Oct4$^+$ (A), Sox1$^+$ Oct4$^-$ (B) and Sox1$^-$ Oct4$^-$ (C) cell counts in wt, *Otx2*$^{-/-}$ and *R26*$^{Otx2/Otx2}$ ESC-derived and EpiSC-derived d5 SFEBs untreated (no factor) or administered with the indicated dosage of BMP4. (**D**) Cell counting of EpiSC colonies derived from d2 BMP4-treated wt and *Otx2*$^{-/-}$ SFEBs. (**E**) Immunostaining for Oct4 and Sox1, and Oct4 and T, performed on *Otx2*$^{-/-}$ EpiSCs cultured in the presence of Fgf2 and activin A and receiving, from p1 to p4, also BMP4 (10 ng/ml). (**F**) Western blots showing that *Otx2*$^{-/-}$ EpiSCs receiving BMP4 at p1 exhibit at p4 only mild expression of Sox1 and a normal level of T. Western blots are normalized by β-actin. Error bars indicate s.d.

in EpiSCs represses neural differentiation and promotes non-neural fate (Zhang et al., 2010). We therefore studied potential functional interactions between Otx2 and BMP4 signaling. First, we administered a high dosage (10 ng/ml) of recombinant BMP4 at d1 to wt and *Otx2*$^{-/-}$ SFEBs and analyzed at d5 Oct4$^+$ Sox1$^-$ (pluripotent), Oct4$^-$ Sox1$^+$ (neural) and Oct4$^-$ Sox1$^-$ (non-neural and non-pluripotent) cell compartments. In *Otx2*$^{-/-}$ SFEBs, BMP4 efficiently repressed neural fate, but was unable to promote non-neural differentiation and caused an expansion of Oct4$^+$ cells (Fig. 8A-C; supplementary material Fig. S11A, Table S9). Importantly, compared with wt, d5 *Otx2*$^{-/-}$ BMP4-treated SFEBs showed increased numbers of Klf4$^+$ Oct4$^+$ ESC-like cells, high expression of *Rex1* and low levels of *Fgf5* transcripts among *Oct4* normalized RNAs (supplementary material Fig. S11A,B). Accordingly, compared with wt, d2 *Otx2*$^{-/-}$ BMP4-treated SFEBs generated many fewer EpiSC colonies when dissociated and cultured in EpiSC medium (Fig. 8D).

To assess the hierarchical position of Otx2 in this process, we analyzed its expression in response to BMP4 or Fgf2 and their inhibitors (DM and PD, respectively) in ESCs cultured in 15% KSR with LIF and in ESCs primed to differentiate in 5% KSR. The Otx2 response was also compared with that of Nanog. Fgf2 induced robust activation of Otx2 in ESCs cultured in 15% KSR with LIF and even stronger activation in those kept in 5% KSR; accordingly, treatment with the Fgf inhibitor PD generated the opposite effect, and treatment with BMP4 or its inhibitor DM revealed a moderate repressive effect of BMP4 on Otx2 expression (supplementary material Fig. S12A-C). The effects on Nanog expression mirrored those on Otx2. Together, these findings suggest that, during the initial ESC transition to EpiSCs, Otx2 antagonizes the inhibitory action of BMP4 through a positive loop with Fgf2 (supplementary material Fig. S11E).

Then, we tested whether BMP4 requires Otx2 to suppress neural fate in SFEBs, this time derived from p0 EpiSC colonies. Compared with wt, the BMP4 antineuralizing activity was less efficient in *Otx2*$^{-/-}$ EpiSC-derived SFEBs (Fig. 8A-C; supplementary material Fig. S11C). We reasoned that if the inefficient neural suppression by BMP4 reflected lack of cooperation with Otx2, then the BMP4 anti-neuralizing activity should be potentiated in *R26*$^{Otx2/Otx2}$ ESC-derived SFEBs. Indeed, *R26*$^{Otx2/Otx2}$ SFEBs cultured with a very low concentration of BMP4 (0.5 ng/ml) that is unable to suppress neural fate in wt

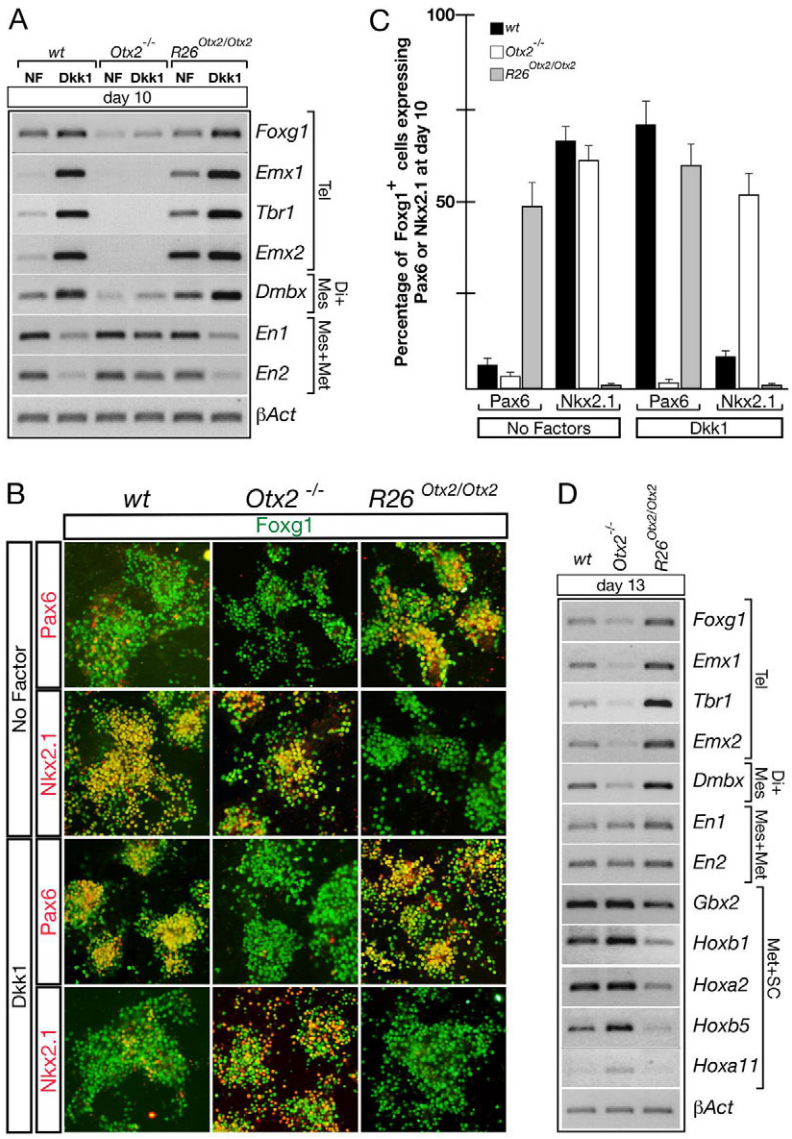

Fig. 9. Otx2 is required for specification of anterior neuroectoderm. (**A**) Wt, *Otx2*$^{-/-}$ and *R26*$^{Otx2/Otx2}$ ESCs induced toward neural differentiation without or with Dkk1 and assayed for the expression of the pan-telencephalic (Tel) marker *Foxg1*, the pallial markers *Emx1*, *Tbr1* and *Emx2*, the diencephalic (Di) and mesencephalic (Mes) marker *Dmbx1*, and the posterior mesencephalic and anterior metencephalic (Met) markers *En1* and *En2*. (**B**,**C**) Immunohistochemistry for Foxg1 and Pax6 and for Foxg1 and Nkx2.1 (B) and cell counting analysis (C) to determine the pallial (Pax6^{+}) and subpallial (Nkx2.1^{+}) identity of Foxg1^{+} cells in wt, *Otx2*$^{-/-}$ and *R26*$^{Otx2/Otx2}$ ESC-derived neural precursors. Error bars indicate s.d. (**D**) Neural differention in adherent monolayer culture conditions shows that, compared with wt, the expression of telencephalic, diencephalic and mesencephalic markers is reduced in *Otx2*$^{-/-}$ and increased in *R26*$^{Otx2/Otx2}$ neural cells, the expression of posterior mesencephalic and rostral metencephalic markers is not substantially affected in *Otx2* mutant cells, and that of metencephalic and spinal cord (SC) markers is increased in *Otx2*$^{-/-}$ and diminished in *R26*$^{Otx2/Otx2}$ neural cells. RT-PCRs are normalized by β-actin.

SFEBs, fully suppressed Sox1^{+} neural cells and generated almost exclusively Oct4^{-} Sox1^{-} cells (Fig. 8A-C; supplementary material Fig. S11D). Accordingly, when *Otx2*$^{-/-}$ EpiSCs induced by Fgf2 and activin A also received BMP4 at p1, the derepression of neural fate was inhibited and EpiSC identity was maintained (Fig. 8E,F). This also suggests that, *in vivo*, the same compensatory mechanism might stabilize the identity of the epiblast of *Otx2*$^{-/-}$ embryos up to gastrulation.

To gain more insight into this aspect, we investigated Otx2 expression in EpiSCs in response to Fgf2, BMP4 and their inhibitors. The expression of Otx2 detected in the presence of Fgf2 and activin A was unaffected by Fgf2 withdrawal or Fgf2 withdrawal and addition of BMP4 (supplementary material Fig. S12D,E). However, treatment with DM in the presence of activin A induced a moderate activation of Otx2, which was enhanced by PD or DM plus PD; of note, Otx2 activation correlated with downregulation of Nanog and Oct4 (supplementary material Fig. S12D,E). Thus, in contrast to ESCs, inactivation of FGF and/or BMP4 signaling in EpiSCs upregulates Otx2 and downregulates pluripotency factors. These data are similar to those reported in human ESCs showing that inhibition of FGF signaling is reflected in OTX2 activation, repression of NANOG and OCT4 and OTX2-mediated activation of PAX6 (Greber et al., 2011). Collectively, these experiments suggest that, in EpiSCs, Otx2 expression is maintained at a relatively low level at which it synergizes with Fgf2 and BMP4 to stabilize the EpiSC state by suppressing neural fate (supplementary material Fig. S11E).

Otx2 requirement for ESC differentiation into anterior neuroectoderm

Previous studies indicated the crucial role played by Otx2 in the specification, regionalization and differentiation of the rostral neuroectoderm (Simeone et al., 2002; Acampora et al., 2009; Simeone et al., 2011). We examined whether the identity of neural progenitors is affected by Otx2. First, we induced the differentiation of neural progenitors enriched in telencephalic precursors (Watanabe et al., 2005). Compared with wt, in *Otx2*$^{-/-}$ neural cells, the expression level of the pan-telencephalic marker Foxg1 was severely diminished, even when telencephalic differentiation should be enhanced by treatment with the WNT antagonist Dkk1; conversely, in *R26*$^{Otx2/Otx2}$ neural progenitors the expression of Foxg1 was moderately increased (Fig. 9A). *Otx2*$^{-/-}$

neural cells retained expression of *En1* and *En2*, and essentially lacked that of telencephalic, diencephalic and mesencephalic markers; conversely, $R26^{Otx2/Otx2}$ neural cells showed increased expression of anterior neuroectoderm markers and attenuated expression of *En1* and *En2* (Fig. 9A).

To assess the subregional identity of presumptive telencephalic precursors we determined the percentage of $Foxg1^+$ cells co-expressing the pallial marker Pax6 and the subpallial marker Nkx2.1. Wt $Foxg1^+$ cells showed a prevalent subpallial ($Nkx2.1^+$) identity, which was converted to pallial by Dkk1 treatment (Fig. 9B,C; supplementary material Table S10). Interestingly, the rare $Otx2^{-/-}$ $Foxg1^+$ patches exhibited a fully penetrant subpallial identity that was unresponsive to Dkk1, whereas $R26^{Otx2/Otx2}$ $Foxg1^+$ cells showed a pallial ($Pax6^+$) identity even in the absence of Dkk1 (Fig. 9B,C).

A different protocol of ESC differentiation into neuroectoderm precursors in adherent monoculture (Ying et al., 2003b) confirmed that lack of Otx2 results in decreased expression of telencephalic, diencephalic and mesencephalic markers and revealed increased expression of metencephalic and spinal cord markers; the opposite expression profile was observed in $R26^{Otx2/Otx2}$ ESC-derived neural cells (Fig. 9D). Thus, these findings indicate that, as in the embryo, Otx2 is crucially required to confer anterior character to ESC-derived neuroectoderm progenitors.

DISCUSSION

Numerous studies have shown that ESC metastability is defined by the opposing and dynamic action of specific signaling pathways and transcription factors (Hanna et al., 2010; Silva and Smith, 2008; Lanner and Rossant, 2010; Niwa, 2007). Signaling molecules such as LIF, but also BMP4 and WNT, together with the transcription factor Nanog, control ground state pluripotency by protecting ESCs from FGF-mediated differentiation commitment (Chambers et al., 2007; Niwa et al., 2009; Ying et al., 2008; ten Berge et al., 2011; Kunath et al., 2007; Niwa, 2011; Wray et al., 2011; Yi et al., 2011; Lyashenko et al., 2011). This antagonism generates in ESCs a continuum of fluctuating and interconvertible states which, if perturbed by genetic modifications or chemical inhibitors, may rapidly drift toward irreversible differentiation or the fully undifferentiated state (Hanna et al., 2010; Niwa, 2007; Silva and Smith, 2008; Lanner and Rossant, 2010; Guo et al., 2009).

In this study, we have investigated for the first time whether Otx2, which has been extensively investigated in the context of brain development, is required in ESCs and EpiSCs. Otx2 is expressed in a large subset of ESCs that defines a cell population showing graded transition from those expressing high levels of Nanog to those exhibiting low or no Nanog expression. ESC culture conditions promoting differentiation (LIF withdrawal and/or Fgf2 addition and/or BMP4 inhibition) induce rapid activation of Otx2, which is prevented by FGF inhibition. Based on these observations, we hypothesized that genetic ablation of *Otx2*, or its constitutive and ubiquitous expression, might affect the ESC state and corrupt the metastable condition. Lack of Otx2 indeed causes severe abnormalities consisting of ubiquitous and constitutive high level expression of Nanog and Klf4, increased LIF signaling and weakened activity of FGF signaling; conversely, constitutive and ubiquitous activation of Otx2 causes a substantial reduction in the number of ESCs co-expressing high levels of Nanog and Klf4, a robust increase of FGF activity, induction of epiblast markers and a very poor ability to generate chimeric embryos. These data strongly suggest that Otx2 is a novel intrinsic determinant of the ESC state, controlling the balance between self-renewal and differentiation. We propose that Otx2 protects the susceptibility to differentiation by counter-balancing signaling pathways and transcription factors that promote ground state pluripotency. Our findings suggest that Otx2 and Nanog, by promoting antagonistic conditions, together contribute to define the ESC metastable state (Fig. 3I). Of note, lack of Otx2, or its ubiquitous activation, generate ESC abnormalities that are similar to those exhibited by ESCs overexpressing or lacking Nanog, respectively (Silva and Smith, 2008; Chambers et al., 2007; Chambers et al., 2003; Mitsui et al., 2003).

This study shows that Otx2 is also required for ESC transition into EpiSCs and maintenance of the EpiSC state. In the absence of any added factor, $Otx2^{-/-}$ ESCs fail the transition to EpiSCs and prematurely differentiate only into neural cells. When provided with Fgf2 and activin A, transition of $Otx2^{-/-}$ ESCs to EpiSCs is initially achieved but maintenance of their state in terms of identity and fate is gradually lost through a progressive mesendoderm-to-neural fate switch accompanied by loss of EpiSC markers, strong activation of Nanog and intense ALP reactivity. Similar abnormalities, with early derepression of neural fate and selective impairment of the endoderm lineage, were also observed in $Otx2^{-/-}$ ESCs induced only with activin A. Thus, Otx2 represents a key factor that is intrinsically required to maintain EpiSC identity, primarily by suppressing neural fate and preventing the adoption of features resembling naïve pluripotency. We speculate that $Otx2^{-/-}$ EpiSCs might progressively regress to an early postimplantation-like epiblast stage, similar to that at which SFEBs prematurely derepress neural fate. In the absence of Otx2, maintenance of EpiSC identity and suppression of neural fate require a high dosage of both Fgf2 and BMP4 in the presence of activin A. Like Fgf2, BMP4 also plays a dual role, first opposing ESC transition into EpiSCs and then suppressing neural fate in EpiSCs (Zhang et al., 2010). Our data suggest that, during the first stage Otx2 antagonizes BMP4-mediated inhibition of EpiSC derivation and, subsequently, in EpiSCs Otx2 synergizes with BMP4 for suppression of neural fate (supplementary material Fig. S11E).

Otx2 has been extensively studied in the context of its essential role in the development and differentiation of anterior neuroectoderm. Our data indicate that Otx2 is crucially required in ESC-derived neural cells to specify the identity of telencephalic and mesencephalic territories and to allow chimerism in the neuroectoderm rostral to the isthmic organizer.

In summary, this study has revealed that Otx2 is a novel determinant controlling the ESC state and its transition to a stable EpiSC condition. Subsequently, as *in vivo*, Otx2 is required to specify the anterior identity of ESC-derived neural progenitors.

Acknowledgements

We thank G. Cossu, T. Perlmann, T. Russo and C. Stern for helpful discussion and constructive criticism; G. Gagliardi for typing and formatting the manuscript; and the confocal microscopy facility of CEINGE Biotecnologie Avanzate.

Funding

This work was supported by the FP6 project for the European Transcriptome, Regulome & Cellular Commitment Consortium (EuTRACC) Integrated Project [LSHG-CT-2007-037445]; the Italian Association for Cancer Research (AIRC) [Project IG – 5499]; the CNR-MIUR Epigenetics Flagship Project; and Regione Campania [L.R.n.5, 2005].

Competing interests statement

The authors declare no competing financial interests.

Author contributions

D.A. performed the experiments and analyzed the data; L.G.D. performed new experiments during the revision; A.S. conceived the experiments, interpreted the data and wrote the paper.

Supplementary material

Supplementary material available online at
http://dev.biologists.org/lookup/suppl/doi:10.1242/dev.085290/-/DC1

References

Acampora, D., Mazan, S., Lallemand, Y., Avantaggiato, V., Maury, M., Simeone, A. and Brûlet, P. (1995). Forebrain and midbrain regions are deleted in Otx2-/- mutants due to a defective anterior neuroectoderm specification during gastrulation. *Development* **121**, 3279-3290.

Acampora, D., Di Giovannantonio, L. G., Di Salvio, M., Mancuso, P. and Simeone, A. (2009). Selective inactivation of Otx2 mRNA isoforms reveals isoform-specific requirement for visceral endoderm anteriorization and head morphogenesis and highlights cell diversity in the visceral endoderm. *Mech. Dev.* **126**, 882-897.

Ang, S. L., Jin, O., Rhinn, M., Daigle, N., Stevenson, L. and Rossant, J. (1996). A targeted mouse Otx2 mutation leads to severe defects in gastrulation and formation of axial mesoderm and to deletion of rostral brain. *Development* **122**, 243-252.

Brons, I. G., Smithers, L. E., Trotter, M. W., Rugg-Gunn, P., Sun, B., Chuva de Sousa Lopes, S. M., Howlett, S. K., Clarkson, A., Ahrlund-Richter, L., Pedersen, R. A. et al. (2007). Derivation of pluripotent epiblast stem cells from mammalian embryos. *Nature* **448**, 191-195.

Chambers, I., Colby, D., Robertson, M., Nichols, J., Lee, S., Tweedie, S. and Smith, A. (2003). Functional expression cloning of Nanog, a pluripotency sustaining factor in embryonic stem cells. *Cell* **113**, 643-655.

Chambers, I., Silva, J., Colby, D., Nichols, J., Nijmeijer, B., Robertson, M., Vrana, J., Jones, K., Grotewold, L. and Smith, A. (2007). Nanog safeguards pluripotency and mediates germline development. *Nature* **450**, 1230-1234.

Di-Gregorio, A., Sancho, M., Stuckey, D. W., Crompton, L. A., Godwin, J., Mishina, Y. and Rodriguez, T. A. (2007). BMP signalling inhibits premature neural differentiation in the mouse embryo. *Development* **134**, 3359-3369.

Di Salvio, M., Di Giovannantonio, L. G., Acampora, D., Prosperi, R., Omodei, D., Prakash, N., Wurst, W. and Simeone, A. (2010). Otx2 controls neuron subtype identity in ventral tegmental area and antagonizes vulnerability to MPTP. *Nat. Neurosci.* **13**, 1481-1488.

Greber, B., Wu, G., Bernemann, C., Joo, J. Y., Han, D. W., Ko, K., Tapia, N., Sabour, D., Sterneckert, J., Tesar, P. et al. (2010). Conserved and divergent roles of FGF signaling in mouse epiblast stem cells and human embryonic stem cells. *Cell Stem Cell* **6**, 215-226.

Greber, B., Coulon, P., Zhang, M., Moritz, S., Frank, S., Müller-Molina, A. J., Araúzo-Bravo, M. J., Han, D. W., Pape, H. C. and Schöler, H. R. (2011). FGF signalling inhibits neural induction in human embryonic stem cells. *EMBO J.* **30**, 4874-4884.

Guo, G., Yang, J., Nichols, J., Hall, J. S., Eyres, I., Mansfield, W. and Smith, A. (2009). Klf4 reverts developmentally programmed restriction of ground state pluripotency. *Development* **136**, 1063-1069.

Hanna, J. H., Saha, K. and Jaenisch, R. (2010). Pluripotency and cellular reprogramming: facts, hypotheses, unresolved issues. *Cell* **143**, 508-525.

Izumi, N., Era, T., Akimaru, H., Yasunaga, M. and Nishikawa, S. (2007). Dissecting the molecular hierarchy for mesendoderm differentiation through a combination of embryonic stem cell culture and RNA interference. *Stem Cells* **25**, 1664-1674.

Kaji, K., Caballero, I. M., MacLeod, R., Nichols, J., Wilson, V. A. and Hendrich, B. (2006). The NuRD component Mbd3 is required for pluripotency of embryonic stem cells. *Nat. Cell Biol.* **8**, 285-292.

Kunath, T., Saba-El-Leil, M. K., Almousailleakh, M., Wray, J., Meloche, S. and Smith, A. (2007). FGF stimulation of the Erk1/2 signalling cascade triggers transition of pluripotent embryonic stem cells from self-renewal to lineage commitment. *Development* **134**, 2895-2902.

Lanner, F. and Rossant, J. (2010). The role of FGF/Erk signaling in pluripotent cells. *Development* **137**, 3351-3360.

LaVaute, T. M., Yoo, Y. D., Pankratz, M. T., Weick, J. P., Gerstner, J. R. and Zhang, S. C. (2009). Regulation of neural specification from human embryonic stem cells by BMP and FGF. *Stem Cells* **27**, 1741-1749.

Linker, C. and Stern, C. D. (2004). Neural induction requires BMP inhibition only as a late step, and involves signals other than FGF and Wnt antagonists. *Development* **131**, 5671-5681.

Lyashenko, N., Winter, M., Migliorini, D., Biechele, T., Moon, R. T. and Hartmann, C. (2011). Differential requirement for the dual functions of -catenin in embryonic stem cell self-renewal and germ layer formation. *Nat. Cell Biol.* **13**, 753-761.

Marks, H., Kalkan, T., Menafra, R., Denissov, S., Jones, K., Hofemeister, H., Nichols, J., Kranz, A., Stewart, A. F., Smith, A. et al. (2012). The transcriptional and epigenomic foundations of ground state pluripotency. *Cell* **149**, 590-604.

Matsuda, T., Nakamura, T., Nakao, K., Arai, T., Katsuki, M., Heike, T. and Yokota, T. (1999). STAT3 activation is sufficient to maintain an undifferentiated state of mouse embryonic stem cells. *EMBO J.* **18**, 4261-4269.

Mitsui, K., Tokuzawa, Y., Itoh, H., Segawa, K., Murakami, M., Takahashi, K., Maruyama, M., Maeda, M. and Yamanaka, S. (2003). The homeoprotein Nanog is required for maintenance of pluripotency in mouse epiblast and ES cells. *Cell* **113**, 631-642.

Miyanari, Y. and Torres-Padilla, M. E. (2012). Control of ground-state pluripotency by allelic regulation of Nanog. *Nature* **483**, 470-473.

Murry, C. E. and Keller, G. (2008). Differentiation of embryonic stem cells to clinically relevant populations: lessons from embryonic development. *Cell* **132**, 661-680.

Najm, F. J., Chenoweth, J. G., Anderson, P. D., Nadeau, J. H., Redline, R. W., McKay, R. D. and Tesar, P. J. (2011). Isolation of epiblast stem cells from preimplantation mouse embryos. *Cell Stem Cell* **8**, 318-325.

Nichols, J. and Smith, A. (2009). Naive and primed pluripotent states. *Cell Stem Cell* **4**, 487-492.

Nichols, J., Silva, J., Roode, M. and Smith, A. (2009). Suppression of Erk signalling promotes ground state pluripotency in the mouse embryo. *Development* **136**, 3215-3222.

Niwa, H. (2007). How is pluripotency determined and maintained? *Development* **134**, 635-646.

Niwa, H. (2011). Wnt: what's needed to maintain pluripotency? *Nat. Cell Biol.* **13**, 1024-1026.

Niwa, H., Ogawa, K., Shimosato, D. and Adachi, K. (2009). A parallel circuit of LIF signalling pathways maintains pluripotency of mouse ES cells. *Nature* **460**, 118-122.

Reynolds, N., Latos, P., Hynes-Allen, A., Loos, R., Leaford, D., O'Shaughnessy, A., Mosaku, O., Signolet, J., Brennecke, P., Kalkan, T. et al. (2012). NuRD suppresses pluripotency gene expression to promote transcriptional heterogeneity and lineage commitment. *Cell Stem Cell* **10**, 583-594.

Rossant, J. (2008). Stem cells and early lineage development. *Cell* **132**, 527-531.

Silva, J. and Smith, A. (2008). Capturing pluripotency. *Cell* **132**, 532-536.

Silva, J., Nichols, J., Theunissen, T. W., Guo, G., van Oosten, A. L., Barrandon, O., Wray, J., Yamanaka, S., Chambers, I. and Smith, A. (2009). Nanog is the gateway to the pluripotent ground state. *Cell* **138**, 722-737.

Simeone, A., Acampora, D., Gulisano, M., Stornaiuolo, A. and Boncinelli, E. (1992). Nested expression domains of four homeobox genes in developing rostral brain. *Nature* **358**, 687-690.

Simeone, A., Puelles, E. and Acampora, D. (2002). The Otx family. *Curr. Opin. Genet. Dev.* **12**, 409-415.

Simeone, A., Puelles, E., Omodei, D., Acampora, D., Di Giovannantonio, L. G., Di Salvio, M., Mancuso, P. and Tomasetti, C. (2011). Otx genes in neurogenesis of mesencephalic dopaminergic neurons. *Dev. Neurobiol.* **71**, 665-679.

ten Berge, D., Kurek, D., Blauwkamp, T., Koole, W., Maas, A., Eroglu, E., Siu, R. K. and Nusse, R. (2011). Embryonic stem cells require Wnt proteins to prevent differentiation to epiblast stem cells. *Nat. Cell Biol.* **13**, 1070-1075.

Tesar, P. J., Chenoweth, J. G., Brook, F. A., Davies, T. J., Evans, E. P., Mack, D. L., Gardner, R. L. and McKay, R. D. (2007). New cell lines from mouse epiblast share defining features with human embryonic stem cells. *Nature* **448**, 196-199.

Toyooka, Y., Shimosato, D., Murakami, K., Takahashi, K. and Niwa, H. (2008). Identification and characterization of subpopulations in undifferentiated ES cell culture. *Development* **135**, 909-918.

Waese, E. Y. and Stanford, W. L. (2011). One-step generation of murine embryonic stem cell-derived mesoderm progenitors and chondrocytes in a serum-free monolayer differentiation system. *Stem Cell Res.* **6**, 34-49.

Watanabe, K., Kamiya, D., Nishiyama, A., Katayama, T., Nozaki, S., Kawasaki, H., Watanabe, Y., Mizuseki, K. and Sasai, Y. (2005). Directed differentiation of telencephalic precursors from embryonic stem cells. *Nat. Neurosci.* **8**, 288-296.

Wray, J., Kalkan, T., Gomez-Lopez, S., Eckardt, D., Cook, A., Kemler, R. and Smith, A. (2011). Inhibition of glycogen synthase kinase-3 alleviates Tcf3 repression of the pluripotency network and increases embryonic stem cell resistance to differentiation. *Nat. Cell Biol.* **13**, 838-845.

Yi, F., Pereira, L., Hoffman, J. A., Shy, B. R., Yuen, C. M., Liu, D. R. and Merrill, B. J. (2011). Opposing effects of Tcf3 and Tcf1 control Wnt stimulation of embryonic stem cell self-renewal. *Nat. Cell Biol.* **13**, 762-770.

Ying, Q. L., Nichols, J., Chambers, I. and Smith, A. (2003a). BMP induction of Id proteins suppresses differentiation and sustains embryonic stem cell self-renewal in collaboration with STAT3. *Cell* **115**, 281-292.

Ying, Q. L., Stavridis, M., Griffiths, D., Li, M. and Smith, A. (2003b). Conversion of embryonic stem cells into neuroectodermal precursors in adherent monoculture. *Nat. Biotechnol.* **21**, 183-186.

Ying, Q. L., Wray, J., Nichols, J., Batlle-Morera, L., Doble, B., Woodgett, J., Cohen, P. and Smith, A. (2008). The ground state of embryonic stem cell self-renewal. *Nature* **453**, 519-523.

Zhang, K., Li, L., Huang, C., Shen, C., Tan, F., Xia, C., Liu, P., Rossant, J. and Jing, N. (2010). Distinct functions of BMP4 during different stages of mouse ES cell neural commitment. *Development* **137**, 2095-2105.

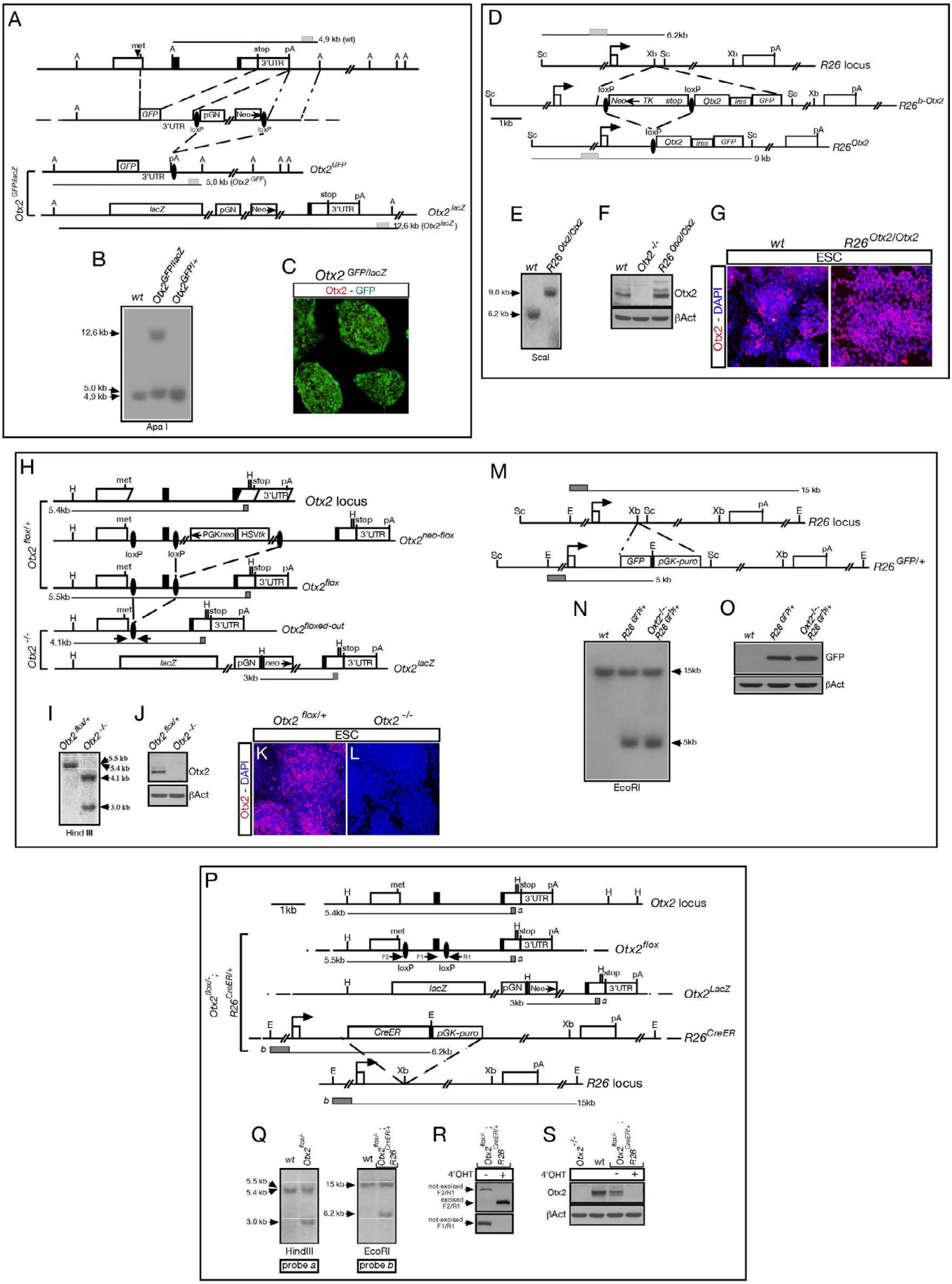
A
met
stop
pA
3'UTR
4,9 kb (wt)
GFP
pGN
Neo
loxP
Otx2 GFP
5,0 kb (Otx2 GFP)
lacZ
Otx2 lacZ
12,6 kb (Otx2 lacZ)
Otx2 GFP/lacZ
B
wt
Otx2GFP/lacZ
Otx2GFP/+
12,6 kb
5.0 kb
4,9 kb
Apa I
C
Otx2 GFP/lacZ
Otx2 - GFP
D
6.2kb
R26 locus
TK
Otx2
ires
GFP
R26 b-Otx2
1kb
R26 Otx2
9 kb
E
wt
R26 Otx2/Otx2
9.0 kb
6.2 kb
ScaI
F
wt
Otx2 -/-
R26 Otx2/Otx2
Otx2
βAct
G
wt
R26 Otx2/Otx2
ESC
Otx2 - DAPI
H
Otx2 locus
5.4kb
PGKneo
HSVtk
Otx2 neo-flox
Otx2 flox
5.5kb
Otx2 floxed-out
4.1kb
Otx2 -/-
Otx2 lacZ
3kb
I
Otx2 flox/+
Otx2 -/-
5.5 kb
5.4 kb
4.1 kb
3.0 kb
Hind III
J
Otx2 flox/+
Otx2 -/-
Otx2
βAct
Otx2 flox/+
Otx2 -/-
ESC
K
L
Otx2 - DAPI
M
15 kb
R26 locus
GFP
pGK-puro
R26 GFP/+
5 kb
N
wt
R26 GFP/+
Otx2 -/- R26 GFP/+
15kb
5kb
EcoRI
O
wt
R26 GFP/+
Otx2 -/- R26 GFP/+
GFP
βAct
P
1kb
Otx2 locus
5.4kb
a
Otx2 flox
5.5kb
F2
F1
R1
loxP
Otx2 LacZ
3kb
CreER
pGK-puro
R26 CreER
b
6.2kb
R26 locus
15kb
Otx2 flox/-; R26 CreER/+
Q
wt
Otx2 flox/-
Otx2 flox/-; R26 CreER/+
5.5 kb
5.4 kb
3.0 kb
15 kb
6.2 kb
HindIII
EcoRI
probe a
probe b
R
4'OHT
- +
not-excised F2/R1
excised F2/R1
not-excised F1/R1
S
Otx2 -/-
Otx2 flox/-; R26 CreER/+
4'OHT
- +
Otx2
βAct

Fig. S1. Generation of *Otx2* mutant ESC lines. (**A**) Schematic representation of the $Otx2^{GFP/lacZ}$ targeting strategy. (**B**) Southern blot of control and mutant ESC lines with the probe corresponding to the gray box in A. (**C**) Immunohistochemistry assay with Otx2 and GFP shows lack of Otx2 and GFP immunoreactivity in $Otx2^{GFP/lacZ}$ ($Otx2^{-/-}$) ESCs. (**D**) Targeting strategy for the $R26^{Otx2}$ allele. (**E**) Southern blot hybridized with the external probe (gray box in D). (**F**) Western blot probed with Otx2 and β-actin antibodies shows that, compared with wt, in $R26^{Otx2/Otx2}$ ESCs the Otx2 total level is approximately doubled. (**G**) Immunohistochemistry assays showing ubiquitous expression of Otx2 in $R26^{Otx2/Otx2}$ ESCs. (**H**) To generate the $Otx2^{-/-};R26^{GFP/+}$ ESC line for chimerism studies, we first inactivated Otx2 through sequential steps required to obtain a new $Otx2^{-/-}$ ESC line without GFP. (**I**) Southern blot hybridized with the external probe (hatched box in H). (**J-L**) Western blots probed with Otx2 and β-actin antibodies (J) and immunohistochemistry assays showing the lack of Otx2 (K,L). (**M**) The $Otx2^{-/-}$ ESC line in H was retransfected to insert the *GFP* gene into one *Rosa26* allele using a GFP, pGK-puro targeting vector; in parallel, E14Tg2a ESCs were transfected only with the GFP targeting construct to generate an $R26^{GFP/+}$ ESC line to be used as control in chimerism studies. (**N**,**O**) Southern and western blot assays of the $R26^{GFP/+}$ and $Otx2^{-/-};R26^{GFP/+}$ mutant ESC lines hybridized with the external probe (hatched box in M) (N), and probed with GFP and β-actin antibodies (O). (**P**) Schematic representation of targeted alleles and sequential steps required to obtain the $Otx2^{flox/-};R26^{CreER/+}$ ESC line. (**Q**) Southern blots hybridized with the *Otx2*-specific external probe *a* and with the *Rosa26*-specific external probe *b* (gray boxes in P). (**R**) Representative PCRs with the indicated primers (horizontal arrows in P) to check *Otx2* DNA excision after 36 hours of exposure to 4-OHT. (**S**) Western blot probed with the Otx2 antibody to show full Otx2 inactivation. β-actin is employed to normalize cell extracts. A, S, X, H, E indicate *Apa*I, *Sca*I, *Xba*I, *Hin*dIII and *Eco*RI, respectively; pA indicates the poly(A) addition site.

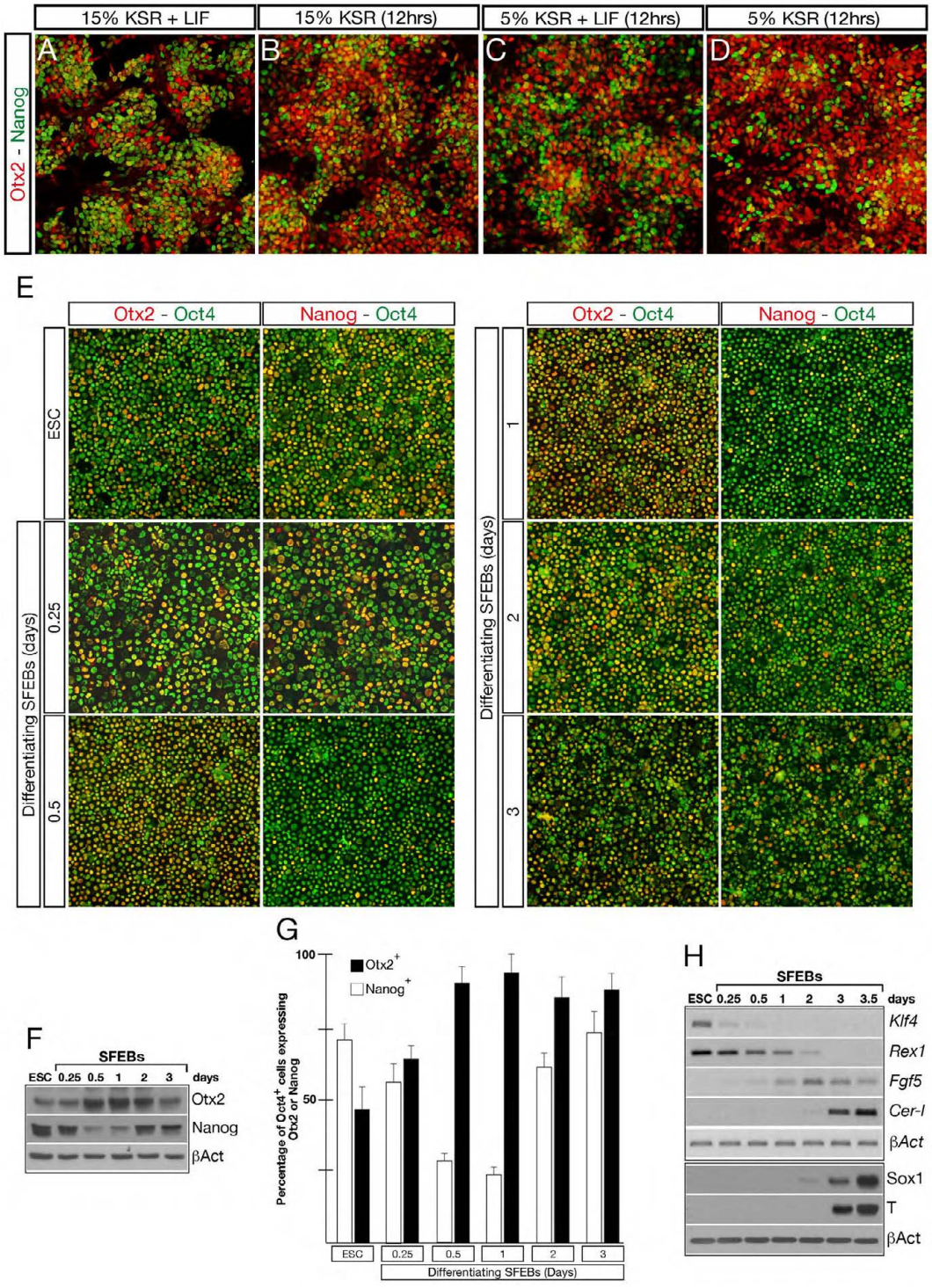

Fig. S2. Otx2 expression is activated by culture conditions favoring differentiation. (**A-D**) Otx2 and Nanog immunohistochemistry assays show that, compared with normal ESC culture conditions (A), LIF withdrawal (B), or diminished concentration of KSR (C) or both LIF withdrawal and reduced concentration in KSR (D) generate a rapid increase in the number of ESCs expressing Otx2 and a corresponding decrease of those expressing Nanog. (**E-G**) Immunohistochemistry experiments (E), western blots (F), and cell-counting analysis (G) show the expression profile (E,F) and the percentage of Oct4^{+} cells co-expressing Otx2 or Nanog at the indicated days (d) of differentiation (G), and reveal that Otx2 expression expands to virtually all Oct4^{+} cells within d1 and mirrors the early reduction in Nanog^{+} cells. (**H**) Western blots and RT-PCR assays show that Otx2 activation mirrors also the extinction of *Klf4* and *Rex1* expression and anticipates the maximal activation of the epiblast markers *Fgf5* and *Cer-l* before differentiation into Sox1^{+} neural and T^{+} mesendoderm cells occurs. β-actin is used to normalize western blots and RT-PCRs.

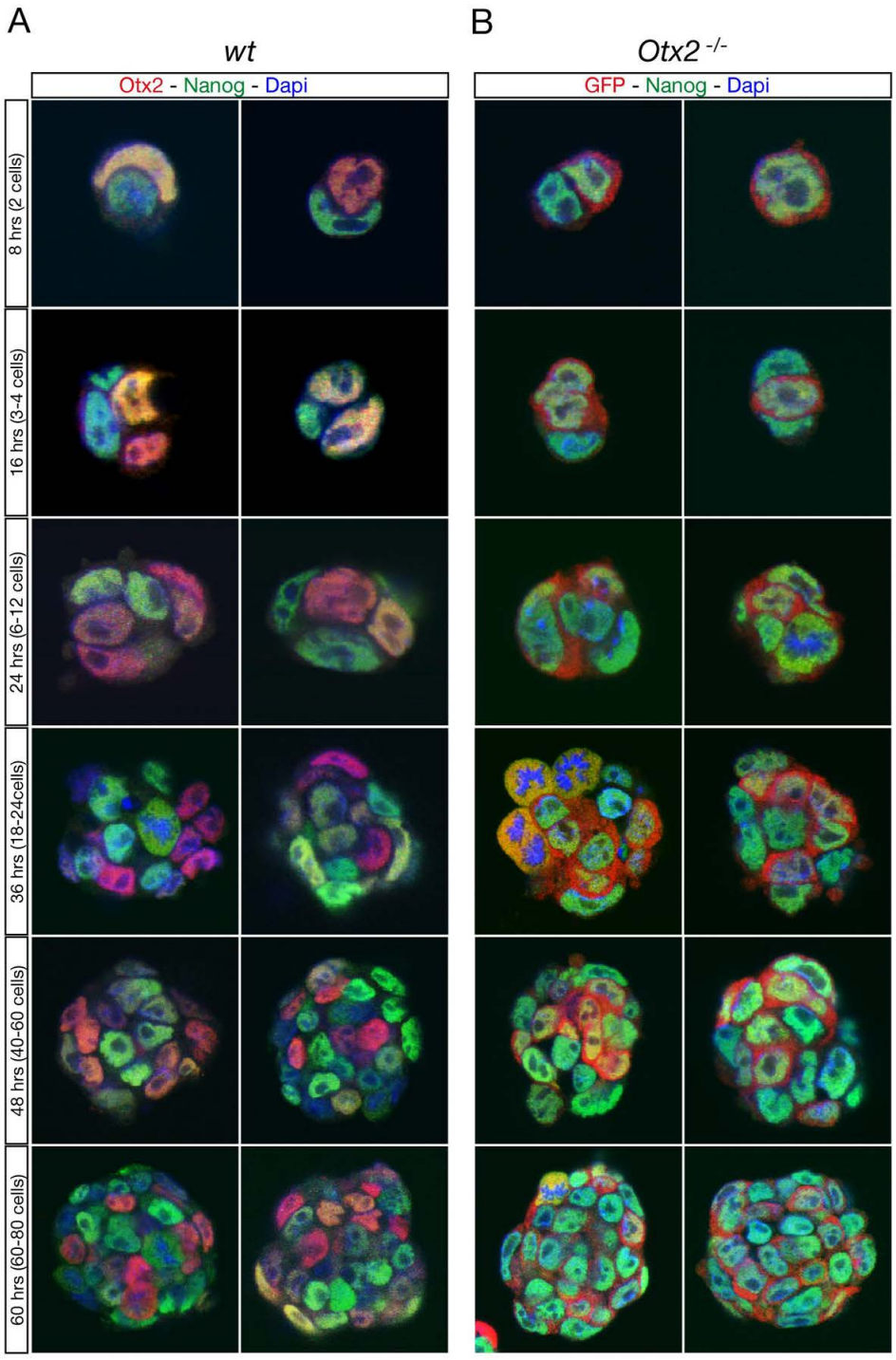

Fig. S3. Lack of Otx2 abolishes cell-to-cell variations of Nanog expression during formation of ESC colonies. Co-immunohistochemistry assays with Otx2 and Nanog, and GFP and Nanog, show that during the early formation of wt ESC colonies since the first cell duplication, Otx2 and Nanog exhibit variable degrees of complementarity and co-expression (**A**); conversely, in *Otx2*$^{-/-}$ ESCs, the expression profile generally observed is characterized by the constitutive high expression of Nanog regardless of the GFP expression (**B**). For each time point, two examples per genotype are shown.

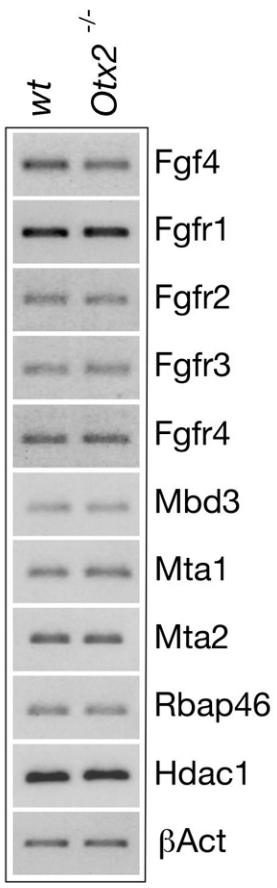

Fig. S4. Expression analysis of Fgf4, Fgf receptors and components of the NuRD complex. Compared with wt, only the expression level of *Fgf4* shows a mild reduction in *Otx2*$^{-/-}$ ESCs, whereas that of *Fgfr1*, *Fgfr2*, *Fgfr3*, *Fgfr4*, *Mbd3*, *Mta1*, *Mta2*, *Rbap46* and *Hdac1* appears unaltered in *Otx2*$^{-/-}$ ESCs.

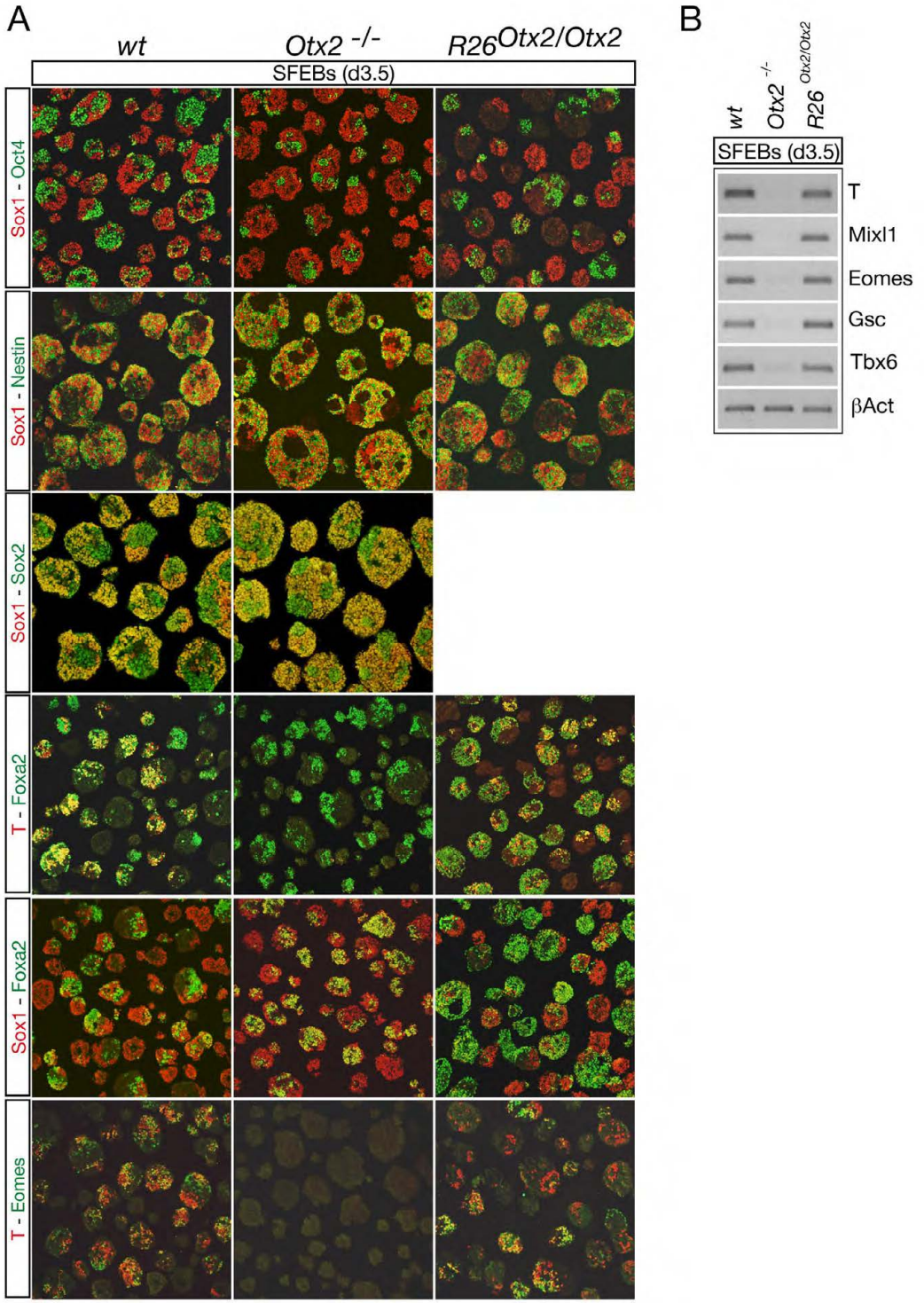

Fig. S5. Otx2 affects cell lineage decisions in differentiating SFEBs. (**A**) Immunohistochemistry experiments on d3.5 wt, *Otx2*$^{-/-}$ and *R26*$^{Otx2/Otx2}$ SFEB sections with Sox1 and Oct4, Sox1 and nestin, Sox1 and Sox2 (only for wt and *Otx2*$^{-/-}$ SFEBs), T and Foxa2, Sox1 and Foxa2, and T and Eomes show that, compared with wt, *Otx2*$^{-/-}$ SFEBs differentiate only in Sox1+ Nestin+ Sox2+ Oct4– neural cells, which are negative for the expression of T and Eomes and fully co-express Foxa2 with Sox1; by contrast, *R26*$^{Otx2/Otx2}$ ESCs generate fewer neural cells, exhibit at d3.5 a number of T^{+} cells similar to that of wt SFEBs, but show a substantial increase in Foxa2^{+} Sox1^{-} presumptive endodermal cells. (**B**) Expression analysis of mesendoderm markers shows that in *Otx2*$^{-/-}$ SFEBs, lack of *T* correlates with loss of *Mixl1*, *Eomes*, *Gsc* and *Tbx6*, whose expression is retained in *R26*$^{Otx2/Otx2}$ SFEBs.

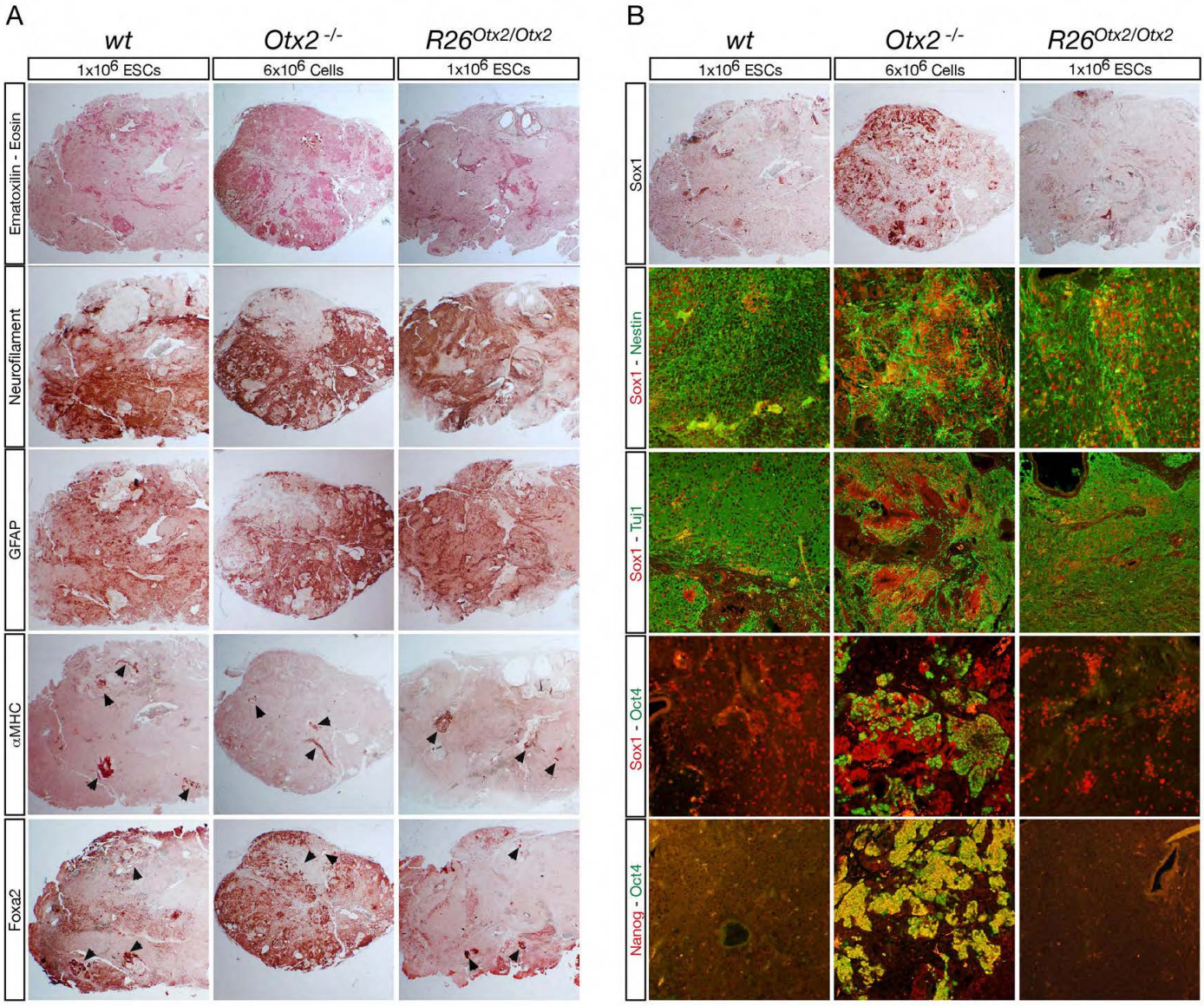

Fig. S6. Differentiation of teratomas generated by *Otx2* mutant ESC lines. (**A**) Wt, *Otx2*$^{-/-}$ and *R26*$^{Otx2/Otx2}$ ESC-derived teratomas generate neuronal and glial cells as revealed by neurofilament and Gfap staining, as well as muscle-like and endodermal-like structures as revealed by αMHC and Foxa2 staining (arrowheads). (**B**) However, *Otx2*$^{-/-}$ ESC-derived teratomas retain unusual enrichment of Sox1^{+} nestin^{+} rosette-like neural progenitors, which differentiate into Tuj1^{+} neurons, and widespread distribution of Oct4^{+} Nanog^{+} pluripotent cell clusters. Note that Oct4^{+} cells frequently co-expressed Sox1.

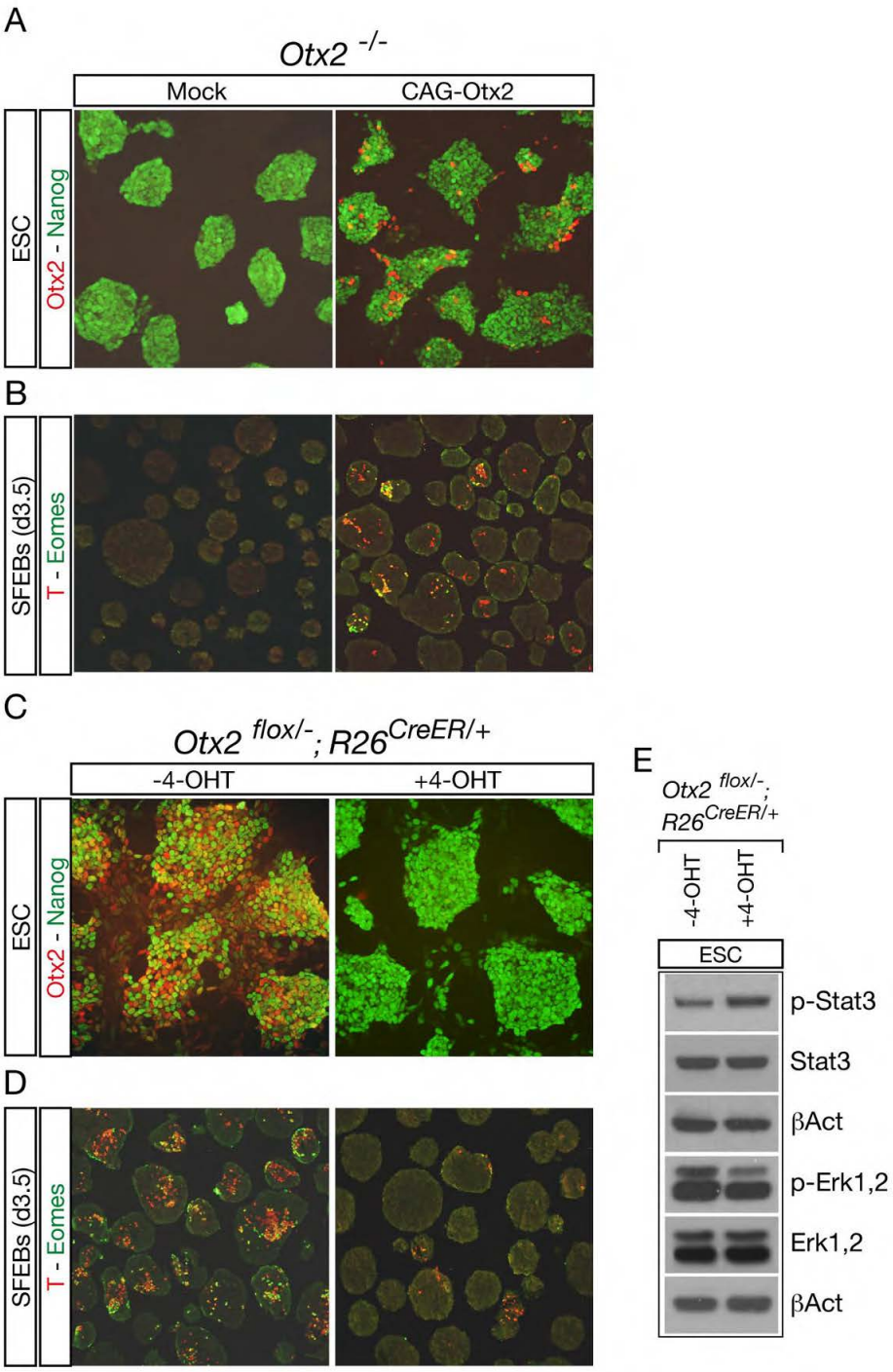

Fig. S7. Phenotypic features of *Otx2*$^{-/-}$ ESCs are not due to adaptation and can be rescued by Otx2 reintroduction. (**A**,**B**) Immunohistochemistry experiments with Otx2 and Nanog on *Otx2*$^{-/-}$ ESCs transfected (48 hours before) or not with the pCAG-Otx2 plasmid (A), and with T and Eomes on *Otx2*$^{-/-}$ d3.5 SFEBs generated from *Otx2*$^{-/-}$ ESCs transfected or not with the pCAG-Otx2 plasmid (B). (**C**,**D**) Immunohistochemistry with Otx2 and Nanog and with T and Eomes, respectively, on *Otx2*$^{flox/-}$;*R26*$^{CreER/+}$ ESCs previously treated or not with 4-OHT (C), and on *Otx2*$^{flox/-}$;*R26*$^{CreER/+}$ SFEBs generated from ESCs previously treated or not with 4-OHT for 3 days (D). (**E**) Western blots to detect the endogenous level of p-Stat3, total Stat3, p-Erk1,2 and total Erk1,2 in *Otx2*$^{flox/-}$;*R26*$^{CreER/+}$ ESCs treated or not for 3 days with 4-OHT. Western blots are normalized by β-actin.

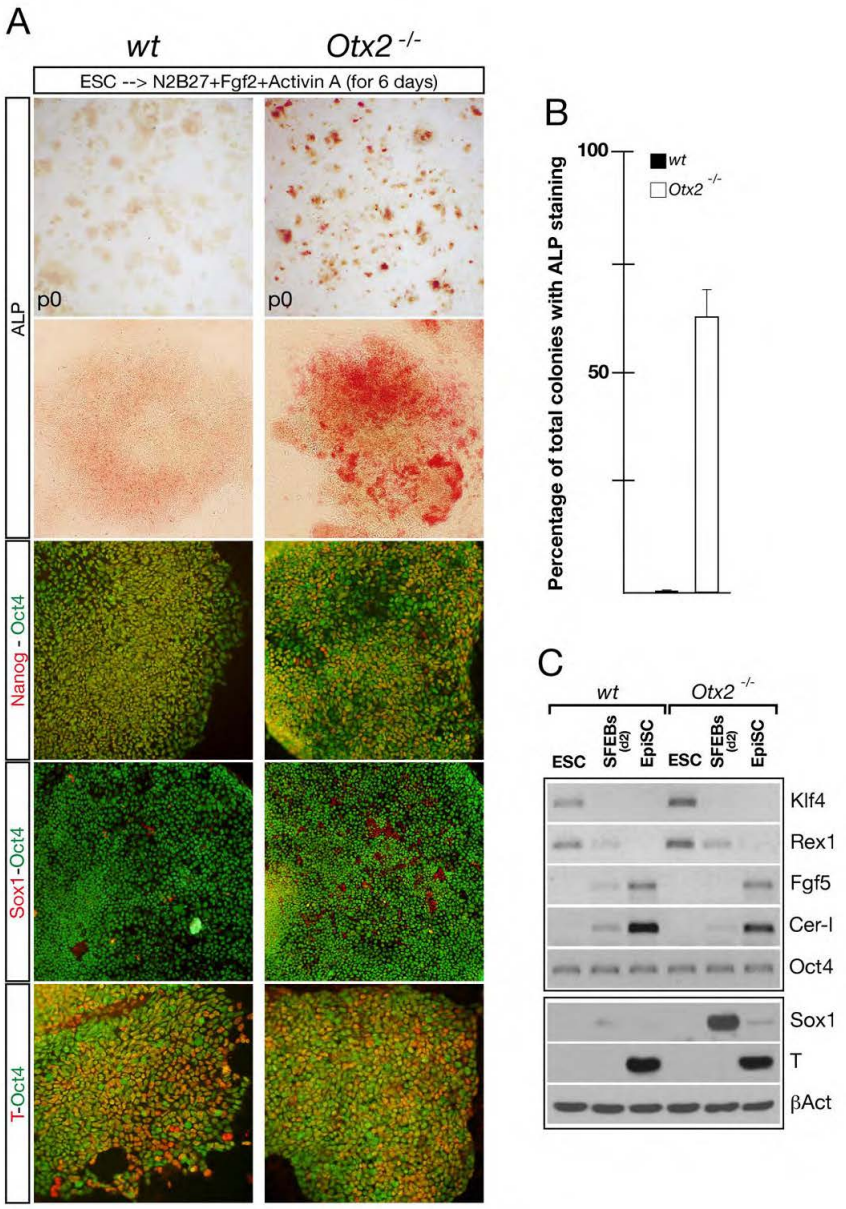

Fig. S8. Fgf2 and activin A induce a fairly normal initial specification of EpiSCs in the absence of Otx2. (**A-C**) Compared with wt, *Otx2*$^{-/-}$ EpiSCs induced for 6 days with Fgf2 and activin A exhibit similar expression for *Fgf5*, *Cer-l*, Sox1 and T (A,C), but show abnormal ALP staining in about 60% of the EpiSC colonies (A,B). RT-PCRs are normalized by *Oct4* and western blots by β-actin.

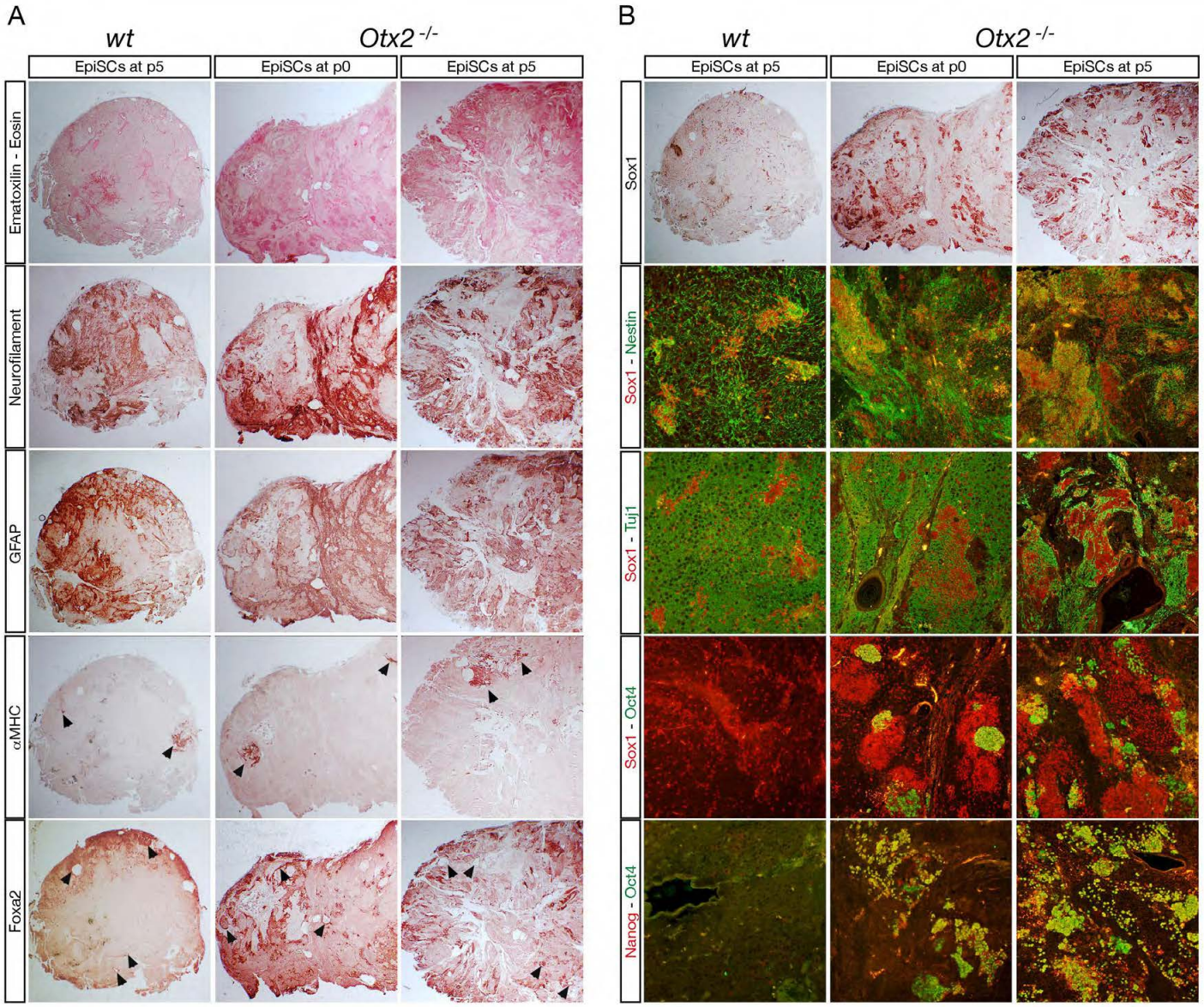

Fig. S9. Differentiation of *Otx2*$^{-/-}$ EpiSC-derived teratomas. (**A**) Compared with p5 wt EpiSC-derived teratomas, those derived from p0 and p5 *Otx2*$^{-/-}$ EpiSCs exhibit neuronal, glial, muscle-like and endodermal-like structures as revealed by neurofilament, Gfap, αMHC (arrowheads) and Foxa2 (arrowheads) staining. (**B**) However, *Otx2*$^{-/-}$ teratomas show numerous Sox1^{+} nestin^{+} rosette-like structures and Oct4^{+} Nanog^{+} cell clusters. Note that the number of Sox1^{+} nestin^{+} and Oct4^{+} Nanog^{+} cell clusters appears increased in teratomas generated by *Otx2*$^{-/-}$ EpiSCs passaged several times.

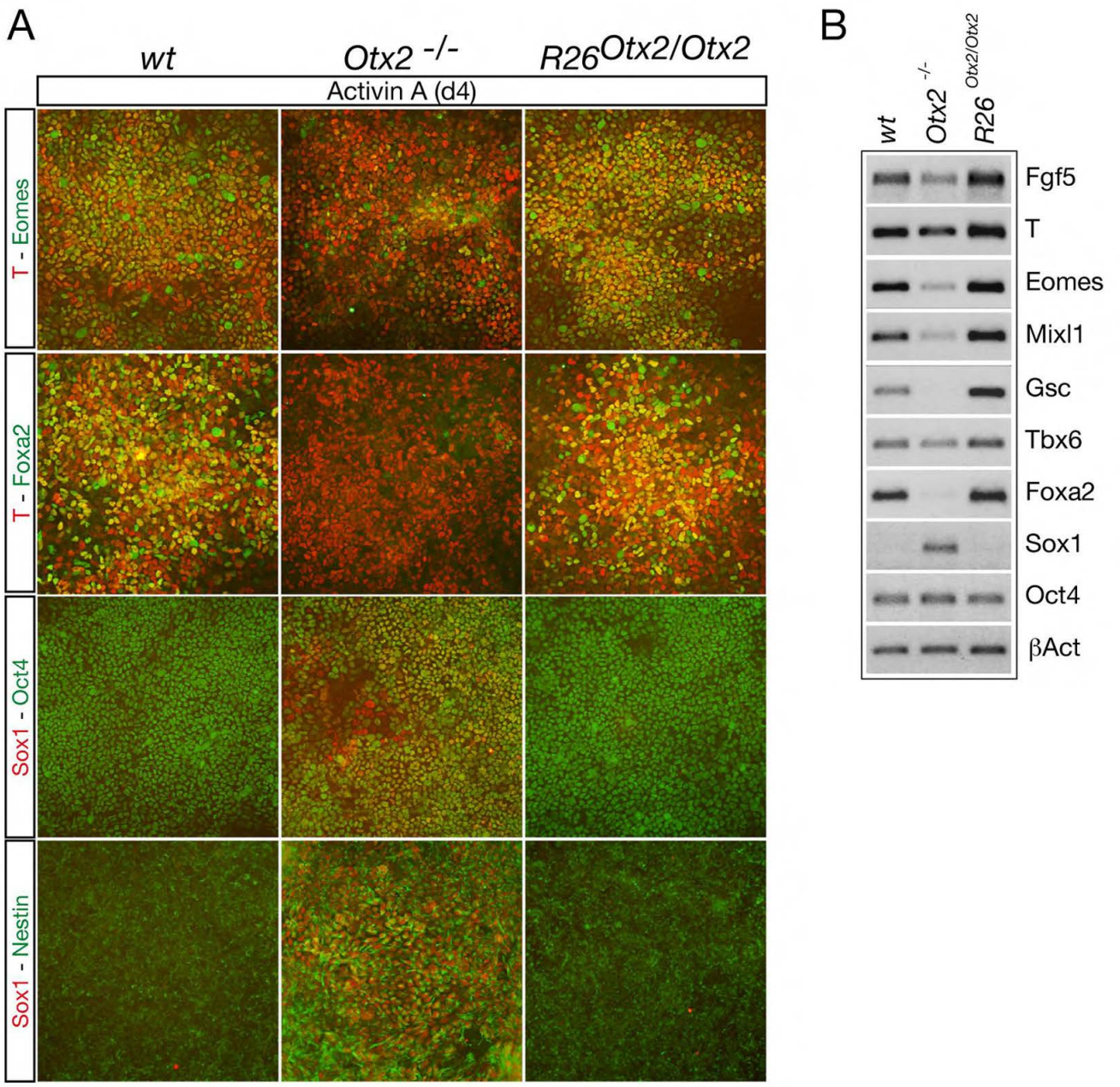

Fig. S10. Mesendoderm induction by activin A is affected in *Otx2*$^{-/-}$ and enhanced in *R26*$^{Otx2/Otx2}$ ESCs. (**A**,**B**) Mesendoderm induction shows that in the absence of Otx2 the expression level of *Eomes*, *Mixl1*, *Gsc* and *Foxa2* is strongly reduced (A,B), *Fgf5* expression is moderately diminished (B), that of *Tbx6* and *T* shows only a mild decrease (A,B), and, importantly, Sox1^{+} nestin^{+} neural progenitors are detected in numerous Oct4^{+} patches (A,B); conversely, the expression of mesendoderm markers is enhanced in *R26*$^{Otx2/Otx2}$ mutant cells (A,B).

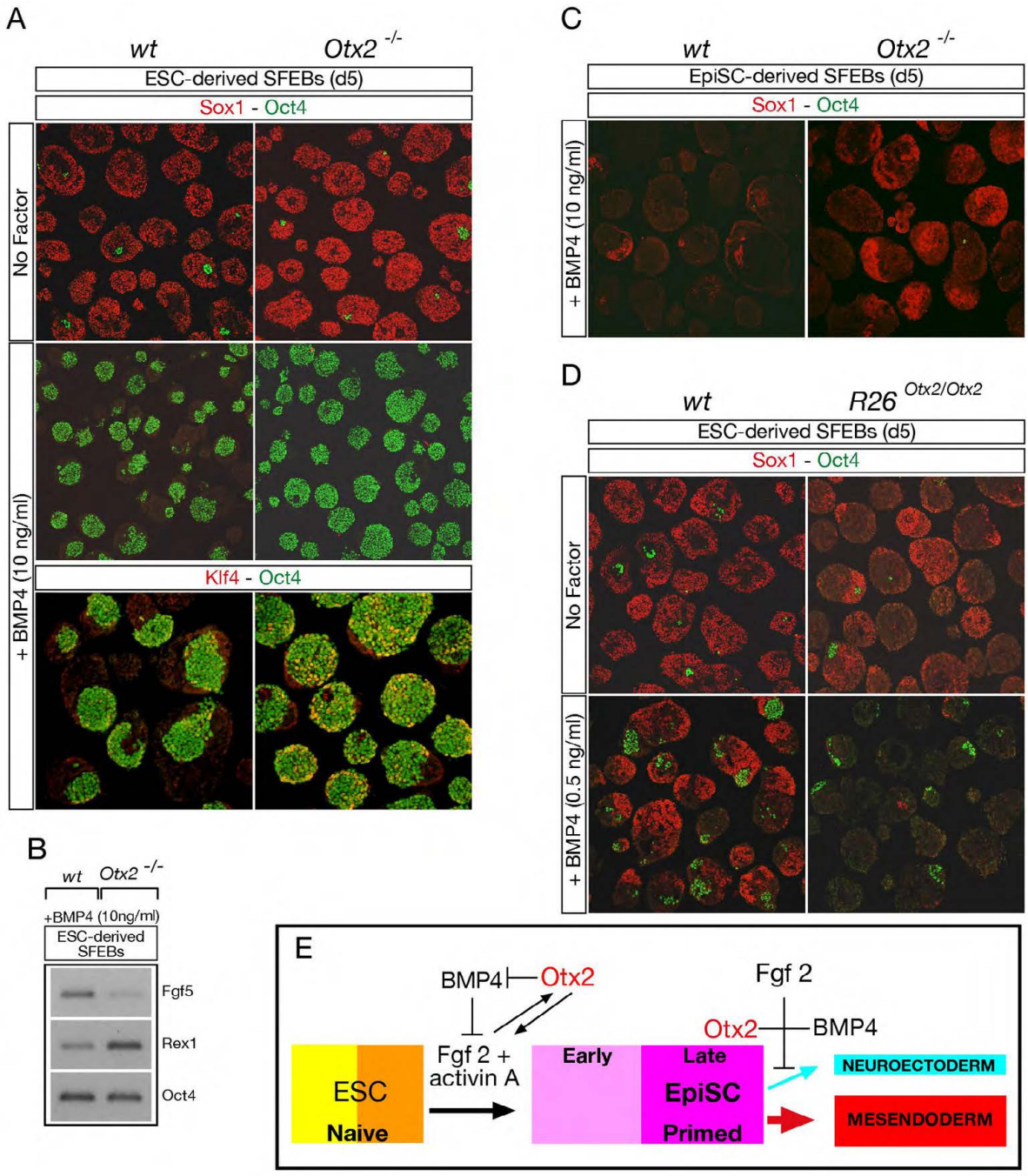

Fig. S11. Otx2 cooperates with BMP4 to suppress neural fate and promote differentiation of non-neural cells. (**A**) Immunohistochemistry assays with Sox1 and Oct4 and Klf4 and Oct4 on d5 wt and *Otx2*$^{-/-}$ ESC-derived SFEBs cultured without (no factor) or with BMP4 show that, compared with wt, *Otx2*$^{-/-}$ SFEBs cultured without BMP4 generate only neural cells, whereas when administered with BMP4 at high dosage (10 ng/ml) *Otx2*$^{-/-}$ SFEBs contain almost exclusively Oct4^{+} pluripotent cells and exhibit a significant increase in Oct4^{+} cells co-expressing the ESC marker Klf4. (**B**) RT-PCR assays showing that in *Otx2*$^{-/-}$ SFEBs the expression of *Rex1* and *Fgf5* is respectively higher and lower than that exhibited by wt SFEBs. RT-PCRs are normalized by *Oct4*. (**C**) Immunohistochemistry assays with Sox1 and Oct4 on wt and *Otx2*$^{-/-}$ EpiSC-derived SFEBs show that, in contrast to wt, high dosage of BMP4 (10 ng/ml) is not sufficient to efficiently suppress neural fate in *Otx2*$^{-/-}$ SFEBs. (**D**) Immunohistochemistry assays with Sox1 and Oct4 on wt and *R26*$^{Otx2/Otx2}$ ESC-derived SFEBs untreated or treated with BMP4 show that, compared with wt, untreated *R26*$^{Otx2/Otx2}$ SFEBs generate fewer Sox1^{+} neural cells and, when administered with a very low dosage of BMP4 (0.5 ng/ml), *R26*$^{Otx2/Otx2}$ SFEBs exhibit a substantial enhancement of the BMP4 anti-neuralizing activity. (**E**) Schematic representation of putative Otx2 actions in ESC transition to EpiSCs and maintenance of the EpiSC condition shows that Otx2 might be involved in the initial priming of ESC transition into EpiSCs by establishing a mutual positive loop with Fgf2 signaling and an antagonism on BMP4 signaling, which, in turn, antagonizes Fgf2-mediated priming. Later, in mature EpiSCs, Otx2 cooperates with Fgf2 and BMP4 to prevent EpiSC instability and the mesendoderm-to-neural fate switch.

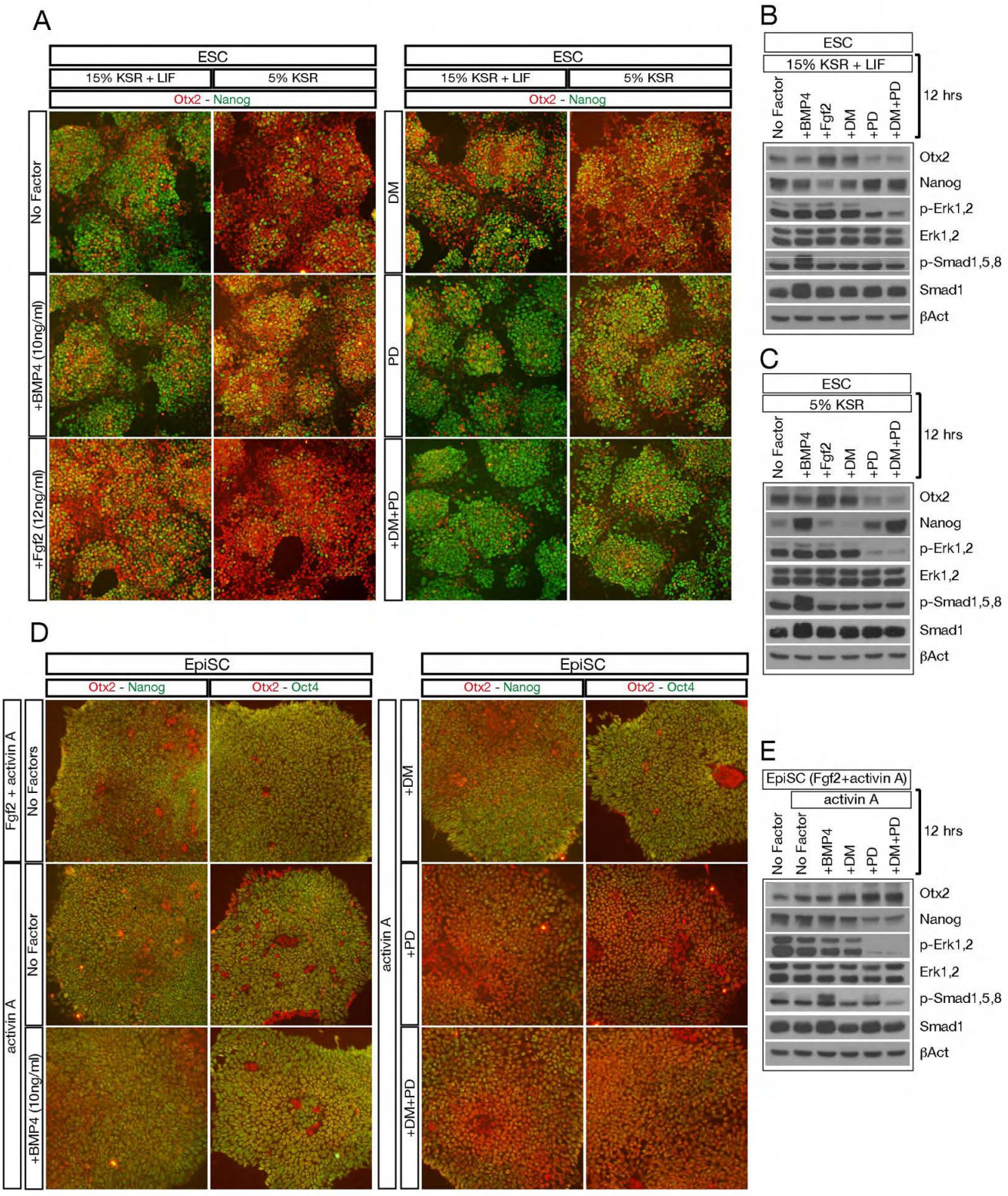

Fig. S12. Otx2 response to Fgf2 and BMP4 factors and their inhibitors. (**A-C**) Otx2 and Nanog expression analyzed by immunohistochemistry (A) and western blotting (B,C) in ESCs cultured in 15% KSR plus LIF without the addition of any factor or inhibitor (no factors) or 12 hours in the presence of BMP4 or Fgf2, or DM or PD, or both DM and PD (A,B); Otx2 and Nanog expression is also analyzed in ESCs cultured for 12 hours in 5% KSR only or with the same factors or inhibitors as for ESCs cultured in 15% KSR+LIF (A,C). (**D**,**E**) Immunohistochemistry with Otx2 and Nanog and Otx2 and Oct4 (D) and western blot analysis with Otx2 and Nanog in EpiSCs induced with Fgf2 and activin A, or Fgf2-deprived and cultured for 12 hours in activin A only or supplemented with BMP4 or DM or PD or both DM and PD (E). The expression level of p-Smad1,5,8, p-Erk1,2, total Erk1,2 and Smad1 is monitored in all experiments (B,C,E) to control the activity of BMP4 and Fgf2 and their inhibitors. β-actin is employed to normalize western blots

Table S1. RT-PCR primers

mRNA	Forward primer	Reverse primer	Size (bp)	N° cycles
β-actin	GGTTCCGATGCCCTGAGGCTC	ACTTGCGGTGCACGATGGAGG	360	18
Klf4	TGCTGAACAGCAGGGACTGTCAC	AGGTGTGCCTTGAGATGAGAACTC	280	24
Rex1	ACTGTGCTGCCTCCAAGTGTTGTC	AGGGAAGCCATCTTCCTCAGTCTC	330	20
Fgf5	TCGGTTTCCATCTGCAGATCTACC	TTCTGTGGATCGCGGACGCATAG	252	22
Cer-l	GTGGAAAGCGATCATGTCTCATCG	GCAAAGGTTGTTCTGGACAACGAC	261	28
Oct4	GCCGACAACAATGAGAACCTTCAG	CGCCGGTTACAGAACCATACTCG	215	22
Fgf4	GCAACGTGGGCATCGGATTC	GTTACCTTCATGGTAGGCGACA	316	25
Fgfr1	GTCACAGCCACTCTCTGCACTG	GACGGAGAAGTAGGTGGTATCGCT	310	26
Fgfr2	GCTCCAATGCAGAAGTGCTGGCTC	GGCAGAACTGTCAACCATGCAGAG	276	28
Fgfr3	GGAGGAGCTGATGGAAACTGATG	GAACAGGACCTTCTCCTGAGGACAG	270	28
Fgfr4	GCTTTGTCCCTTGAGGCCTCTGAG	GTATCGGCCAGCATCCTCAGGAAG	243	28
Mta1	CAAGTCGGAATCTCCTGCTCAATG	GGCGCAGGGCAATGGGTTTGTAGG	225	25
Mta2	GAGAACTCCTCCAGCAATCCTTAC	GTGGCTGGTAATGATTCAAACTGC	255	25
Hdac1	CCTCACAAAGCCAATGCTGAGGAG	GTTCACAGCGATGTCCGTCTGCTG	237	27
Rbap46	GAAGATACTGTGGAGGAGCGTGTC	CATCAAACTGTGCATCATCATTGG	260	25
Mbd3	TTCCAGGTCTCAGTGCAGGGA	TGACTTCCTGGTGGGCTGCT	334	25
T	CACCAGCATGCTGCCTGTGAGTCA	CTGGCTGTCAGAAATGTCTGTGAC	264	27
Goosecoid	TCTTCACCGATGAGCAGCTCGAAG	CAGCTGTCCGAGTCCAAATCGCT	276	29
Eomes	GCTTCAACATAAACGGACTCAACC	GTTCATTCAAGTCCTCCACACCGT	344	27
Mixl1	AGTTGCTGGAGCTCGTCTTCCGA	ATCCGGAACGTGGTTCACATCTG	266	27
Tbx6	GCTTCCTCTCTGGGATCGAGGCAG	CCTCTGGGTCCAGGCCAGTGACTG	264	28
Foxg1	ACTTTGAGTTACAACGGGACCACG	AAAGTAACTGGTCTGGCCCGC	282	27
Emx2	ACGACACAAGTCCCGAGAGTTTCC	TGCTTGGTAGCAATTCTCCACCG	310	28
Dmbx1	CCATCAGTGCATGCGCTTACGTT	GGCAAACCAGGAGGCTGTTCTG	399	29
En1	CAACCCTGCGATCCTACTCATGG	GATATAGCGGTTTGCCTGGAACTC	247	29
Gbx2	ATGGCGCTCACCTCCACGCTCAT	CATCTGAGCTGTAATCCACATCG	340	28
Sox1	GCACCAAGGCCAACCAGGATCGG	TTCTTGAGCAGCGTCTTGGTCTTG	268	27
Hnf3b	TCCGACTGGAGCAGCTACTACG	TCAGACTCGGACTCAGGTGAGGTC	300	27
Emx1	CAGGACGGGCTGCTTTTGCACG	GTGACATCAATGTCCTCCCCGTTG	326	30
Tbr1	GGAGACTCAGTTCATCGCTGTCA	CTTGGCGTAGTTGCTCACGAACTG	241	30
En2	TCCGACTCGGACAGCTCTCAAG	TCTTGATCTAGACTCGTTCAGG	280	29
Hoxa2	CCTGCCTGCCTCGGCCACAAAG	CACTGGGTTTGCCTCTTATGCTTC	242	31
Hoxa11	CACACTGAGGACAAGGCCGGTG	CCCTCCCAATTCCAGTAGGCTGG	270	33
Hoxb1	CAACCTTTGCATCAGCCTACGAC	CACCTGCGTTTCATTGAGCTCCA	290	32
Hoxb5	GCCAATTTCACCGAAATAGACGAG	ATCTGACGCTCGGACAGGCAAAG	330	33

Table S2. ESC subsets co-expressing Otx2 and Nanog

Genotype	N° of Exp.	ESC subpopulations co-expressing different levels of Otx2 and Nanog								
		Total $Otx2^{+}$ cells	$Otx2^{+}$ $Nanog^{h+m}$	$Otx2^{+}$ $Nanog^{l+a}$	Total $Otx2^{h+m}$	$Otx2^{h+m}$ $Nanog^{h+m}$	$Otx2^{h+m}$ $Nanog^{l+a}$	Total $Otx2^{l+a}$	$Otx2^{l+a}$ $Nanog^{h+m}$	$Otx2^{l+a}$ $Nanog^{l+a}$
wt	4	1436±201	672±55	736±149	625±63	234±23	398±54	399±50	261±23	138±28

h, m, l or a indicate high, moderate, low or absent expression, respectively; $Otx2^{+}$ or $Nanog^{+}$ indicate ESCs expressing the indicated factor regardless of the expression level.

Table S3. Total Oct4^{+} cells and Oct4^{+} cells co-expressing Nanog or Otx2 in ESCs and SFEBs

Genotype	No of Exp.	Time course (hours)	Total Oct4^{+} cells and Oct4^{+} subtypes expressing Nanog or Otx2 (mean ± s.d.)					
			Total cells	Oct4^{+}	Total Oct4^{+} cells	Oct4^{+} Nanog^{+}	Total Oct4^{+} cells	Oct4^{+} Otx2^{+}
wt	4	0 (ESC)	*	*	2813±125	1991±138	2770±286	1281±191
wt	4	6	*	*	2613±232	1472±154	2338±285	1496±128
wt	4	12	*	*	2930±142	824±64	3261±182	2901±206
wt	4	24	*	*	2566±243	622±80	2742±214	2555±192
wt	4	48	2643±108	2459±145	2995±301	1828±137	3255±165	2728±243
wt	4	72	2709±136	1935±104	2067±167	1503±141	2127±149	1856±112
wt	4	90	2423±94	1197±109	**	**	**	**
Otx2$^{-/-}$	4	0 (ESC)	*	*	**	**	n/a	n/a
Otx2$^{-/-}$	4	12	*	*	**	**	n/a	n/a
Otx2$^{-/-}$	4	24	*	*	**	**	n/a	n/a
Otx2$^{-/-}$	4	48	3207±39	1922±198	**	**	n/a	n/a
Otx2$^{-/-}$	4	72	3212±202	1223±188	**	**	n/a	n/a
Otx2$^{-/-}$	4	90	3904±431	664±138	**	**	n/a	n/a
R26$^{Otx2/Otx2}$	4	0 (ESC)	3024±169	2393±190	**	**	n/a	n/a
R26$^{Otx2/Otx2}$	4	12	3125±131	2566±154	**	**	n/a	n/a
R26$^{Otx2/Otx2}$	4	24	3131±149	2337±166	**	**	n/a	n/a
R26$^{Otx2/Otx2}$	4	48	2965±162	1986±126	**	**	n/a	n/a
R26$^{Otx2/Otx2}$	4	72	2859±95	1459±154	**	**	n/a	n/a
R26$^{Otx2/Otx2}$	4	90	4980±332	1407±150	**	**	n/a	n/a

*At 6, 12 and 24 hours all cells were Oct4^{+} in wt and *Otx2*$^{-/-}$ ESC lines and differentiating SFEBs.
**Not determined.

Table S4. ALP in wt and *Otx2* mutant ESC colonies

		Undifferentiated ESC colonies ($\times 10^3$ plated ESCs) (mean ± s.d.)		
Genotype	**N° of Exp.**	**Uniform ALP$^+$ (+LIF)**	**Uniform ALP$^+$ (–LIF)**	**Uniform ALP$^+$ (–LIF+JAK inh.)**
wt	4	232±39	6±4	0
Otx2$^{-/-}$	4	823±66	311±61	124±30
R26$^{Otx2/Otx2}$	4	72±16	n/a	n/a

Table S5. Oct4, Nanog and Klf4 in wt, *Otx2*$^{-/-}$ and *R26*$^{Otx2/Otx2}$ ESCs

		Oct4, Nanog and Klf4 ESC subsets (mean ± s.d.)					
Genotype	**N° of Exp.**	**Total cells**	**Oct4^{+}**	**Total cells**	**Nanog^{+}**	**Total cells**	**Klf4^{+}**
wt	4	*	*	2630±127	1863±142	2328±71	1508±138
Otx2$^{-/-}$	4	*	*	2587±125	2444±131	2235±83	2036±142
R26$^{Otx2/Otx2}$	4	3024±169	2393±190	2606±133	1410±107	2446±237	437±87

*All cells were Oct4^{+} in wt and *Otx2*$^{-/-}$ ESCs.

Table S6. Chimeric embryos generated by control and *Otx2* mutant ESCs

Genotype	Injected embryos	Recovered embryos	Chimerism			
			High	Moderate	Low	Undetectable or very low
$R26^{GFP/+}$	76	65	39	16	6	4
$Otx2^{-/-};R26^{GFP/+}$	83	61	26	22	11	2
$R26^{Otx2/Otx2}$	105	78	0	0	13	65

Table S7. Teratoma occurrence in wt and *Otx2* mutant ESCs and EpiSCs

Genotype	Number of subcutaneous injections	Number of injected ESCs	Number of injected EpiSCs	Recovered teratomas	Size*		
					Large (>0.7 cm)	Small (<0.5 cm)	Undetectable
$R26^{GFP/+}$	12	1.5×10^6		12	10	2	0
$Otx2^{-/-};R26^{GFP/+}$	11	1.5×10^6		2	0	2	9
$Otx2^{-/-};R26^{GFP/+}$	10	6×10^6		6	1	5	4
$R26^{Otx2/Otx2}$	12**	1.5×10^6		10	8	2	1
$R26^{GFP/+}$	6		1.5×10^6	4	4	0	2
$Otx2^{-/-};R26^{GFP/+}$	8		1.5×10^6	7	4	3	1

*The size classification was based on the largest diameter after mid-sectioning of the teratomas.
**One of the injected mice died prematurely.

Table S8. Wt, *Otx2*$^{-/-}$ and *R26*$^{Otx2/Otx2}$ neural and mesendoderm cell lineages in SFEBs at d3.5

			Number of neural and mesendodermal cells (mean ± s.d.)					
Genotype	**N° of Exp.**	**Factor (ng/ml)**	**Total cells**	**Sox1^{+}**	**Total cells**	**T^{+}**	**Total cells**	**Sox1^{-} Foxa2^{+}**
wt	4	None	4218±575	2151±293	3857±383	679±184	3061±358	805±142
Otx2$^{-/-}$	4	None	3982±467	3464±273	n/a	n/a	n/a	n/a
R26$^{Otx2/Otx2}$	4	None	4780±576	1496±246	5342±349	1199±264	3951±149	2343±268

Table S9. Pluripotent, neural and non-neural cells in wt and *Otx2* mutant SFEBs derived from ESCs or EpiSCs

			Number of Oct4$^+$, Sox1$^+$ and Sox1$^-$ Oct4$^-$ cells in SFEBs at day 5 (mean ± s.d.)			
Genotype	**N° of Exp.**	**BMP4 (ng/ml)**	**Total cells**	**Oct4$^+$**	**Sox1$^+$**	**Sox1$^-$ Oct4$^-$**
wt ESC-derived SFEBs	4	—	4974±336	77±18	3730±314	1166±239
Otx2$^{-/-}$ ESC-derived SFEBs	4	—	4595±298	51±25	4357±231	202±108
R26$^{Otx2/Otx2}$ ESC-derived SFEBs	4	—	4240±303	44±10	1191±179	3005±183
wt ESC-derived SFEBs	4	10	5037±663	2450±266	9±3	2576±421
Otx2$^{-/-}$ ESC-derived SFEBs	4	10	4912±578	4213±333	12±7	686±265
wt ESC-derived SFEBs	4	0.5	3987±375	514±86	1943±236	1529±283
R26$^{Otx2/Otx2}$ ESC-derived SFEBs	4	0.5	4013±469	234±84	115±47	3688±281
wt EpiSC-derived SFEBs	4	10	6398±135	13±3	373±136	6021±252
Otx2$^{-/-}$ EpiSC-derived SFEBs	4	10	6478±181	17±4	1735±263	4736±331

Table S10. Pallial and sub-pallial differentiation in wt, *Otx2*$^{-/-}$ and *R26*$^{Otx2/Otx2}$ neural differentiation

			Number of Foxg1^{+} cells co-expressing pallial or sub-pallial markers (mean ± s.d.)			
Genotype	**N° of Exp.**	**Factor (ng/ml)**	**Total Foxg1^{+}**	**Pax6^{+} Foxg1^{+}**	**Total Foxg1^{+}**	**Nkx2.1^{+} Foxg1^{+}**
wt	4	None	1337±125	84±23	1407±146	930±55
Otx2$^{-/-}$	4	None	566±118	18±5	641±108	391±24
R26$^{Otx2/Otx2}$	4	None	1507±136	744±104	1491±125	18±8
wt	4	Dkk1 (500 ng/ml)	1531±145	1069±107	1418±109	131±30
Otx2$^{-/-}$	4	Dkk1 (500 ng/ml)	941±72	21±9	938±70	494±57
R26$^{Otx2/Otx2}$	4	Dkk1 (500 ng/ml)	1509±169	886±96	1493±161	15±5